Development and Characterization of DNA-based Kit for Cancer Diagnosis

Author

Areej Fatima

Regn Number

361869

Supervisor

Dr. Adeeb Shehzad

BIOMEDICAL ENGINEERING AND SCIENCES

SCHOOL OF MECHANICAL & MANUFACTURING ENGINEERING

NATIONAL UNIVERSITY OF SCIENCES AND TECHNOLOGY

ISLAMABAD

JULY (2023)

I

Development and Characterization of DNA-based Kit for Cancer Diagnosis

Author

Areej Fatima

Regn Number

361869

A thesis submitted in partial fulfillment of the requirements for the degree of

MS Biomedical Sciences

Thesis Supervisor:

Dr. Adeeb Shehzad

Thesis Supervisor's Signature: _____

BIOMEDICAL ENGINEERING AND SCIENCES

SCHOOL OF MECHANICAL & MANUFACTURING ENGINEERING

NATIONAL UNIVERSITY OF SCIENCES AND TECHNOLOGY,

ISLAMABAD
JULY 2023

II

National University of Sciences & Technology

MASTER THESIS WORK

We hereby recommend that the dissertation prepared under our supervisio

by: Areej Fatima   Reg no# 361869

Titled: Development and characterization of DNA-based kit for cancer diagnosis

be accepted in partial fulfillment of the requirements for the award of MS degree.

Examination Committee Members

1.   Name: Dr. Syed Omer Gilani   Signature: _____

2.   Name: Dr. Aneeqa Noor   Signature: _____

3.   Name: Dr. Zia Mohy Ud Din   Signature: _____

Supervisor's name: Dr.Adeeb Shehzad   Signature: _____

Date: 11/7/2023

_____   12-7-23
Head of Department   Date

COUNTERSINGED
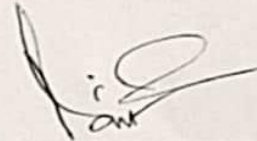
Dean/Principal

Date: 19-7-2023

THESIS ACCEPTANCE CERTIFICATE

Certified that the final copy of the MS thesis written by **Ms. Areej Fatima (Registration No. 361869)**, of SMME (School of Mechanical and Manufacturing Engineering) has been vetted by the undersigned, found complete in all respects as per NUST Statutes / Regulations, is within the similarity indices limit and is accepted as partial fulfillment for the award of MS/MPhil degree. It is further certified that necessary amendments as pointed out by GEC members of the scholar have also been incorporated in the said thesis.
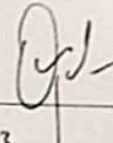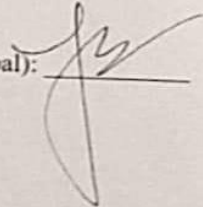
Signature: _____

Name of Supervisor: Dr. Adeeb Shehcad

Date: 11-7-2023

Signature (HOD): _____
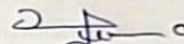
Date: 12-7-23

Signature (Dean/Principal): _____

Date: 19-7-2023

Declaration

Declaration

I certify that this research work titled *"Development and Characterization of DNA-based Kit for Cancer Diagnosis"* is my own work. The work has not been presented elsewhere for assessment. The material that has been used from other sources has been properly acknowledged / referred.

Signature of Student

Areej Fatima

2021-NUST-Ms-BMS-361869
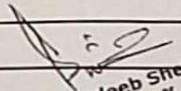
III

Plagiarism Certificate

Proposed Certificate for Plagiarism

It is certified that PhD/M.Phil/MS Thesis Titled Development and Characterization of DNA-based Kit for Cancer Diagnosis by Areej Fatima has been examined by us. We undertake the follows:

a. Thesis has significant new work/knowledge as compared already published or are under consideration to be published elsewhere. No sentence, equation, diagram, table, paragraph or section has been copied verbatim from previous work unless it is placed under quotation marks and duly referenced.

b. The work presented is original and own work of the author (i.e. there is no plagiarism). No ideas, processes, results or words of others have been presented as Author own work.

c. There is no fabrication of data or results which have been compiled/analyzed.

d. There is no falsification by manipulating research materials, equipment or processes, or changing or omitting data or results such that the research is not accurately represented in the research record.

e. The thesis has been checked using TURNITIN (copy of originality report attached) and found within limits as per HEC plagiarism Policy and instructions issued from time to time.

Name & Signature of Supervisor

Signature :

Dr. Adeeb Shehzad
Associate Professor
Department of Biomedical Engg & Sciences
School of Mechanical & Manufacturing
Engineering (SMME), NUST
Islamabad

Copyright Statement

Acknowledgments

Dedicated to my exceptional parents and adored siblings whose tremendous support and cooperation led me to this wonderful accomplishment

Abstract

Cancer impermanence and the incidence rate is increasing gradually. Cancer costs us not only economically but also our beloved ones. Different treatments are available to combat cancer propagation. The effectiveness of the treatment is directly related to the diagnosis of cancer. The earlier the cancer diagnosis, the earlier the treatment begins. Various types of diagnostic methods for cancer are available, but all those deal with the later stages of cancer. Moreover, they are specific to one type of cancer. In this study, we tried to design a biosensor that can detect cancer at its earlier stages. The biosensor simply consists of graphene that acts as a transistor, a linker that makes the connection between the graphene and antibodies that capture the biomarker of cancer. Metal electrodes are present at both ends of the graphene. We immobilized the antibodies on the sensor, but we haven't attained the current-voltage shift produced in response to the binding of cancer biomarkers to the antibodies. A lot remains yet to explore in this domain.

Keywords: Cancer, Graphene, Linker, Antibodies, Kit, Detection

Tables of Contents

List of Abbreviation

- ACS - American Cancer Society

- PSA - Prostate-Specific Antigen

- CA125 - Cancer Antigen 125

- CEA - Carcinoembryonic Antigen

- BPH - Benign prostatic hyperplasia

- CSF - Cerebrospinal fluid

- AFP - Alpha-Fetoprotein

- HCC - Hepatocellular carcinoma

- AASLD -Association for the Study of Liver Disease

- EASL -European Association for the Study of the Liver

- β-HCG - Beta Subunit HCG

- CT - Computed Tomography

- MRI - Magnetic Resonance Imaging,

- PET -Positron Emission Tomography

- GFET -Graphene Field-Effect Transistor

- RIA -Radioimmunoassay

- circRNAs - Circular RNAs

- TME - Tumor Microenvironment

- EMT- Epithelial-Mesenchymal Transition

- CVD - Chemical Vapor Deposition

- Hcg -Human Chorionic Gonadotropin

- V CNP- Dirac-point gate voltage

- XPS - X-ray Photoelectron Spectroscopy

- S1-Ag - SARS-CoV-2 Spike S1 antigen.

- ADH - Anti-Diuretic Hormone

- NDI - Nephrogenic Diabetes Insipidus

- SEM - Scanning Electron Microscopy
- FTIR - Fourier Transformed infrared spectroscopy.

- PVP - Polyvinylpyrrolidone
- SiO_2 -Silicon dioxide

- CMC -Carboxymethylcellulose

- G - Graphene

- GL - Linker Attached to Graphene

- GLA - Antibody Attached to Graphene via Linker

List of Figures and Tables

Chapter 1: Introduction

Cancer is a condition where cells in the body grow out of control and can spread to other parts. Normally, our cells grow, divide, and replace old ones as needed. But when something goes wrong, damaged cells can start to grow and form lumps called tumors. Tumors can be either cancerous or non-cancerous). The cancerous tumors have the ability to invade nearby tissues and even metastasize to other parts of the body [1]. Benign tumors usually stay in one place and don't spread, but they can still cause problems if they grow too large [2, 3]. Cancer is classified as a genetic disorder, wherein alterations to genes governing cellular functionality, particularly in terms of growth and division, serve as the primary causative factors [3]. Genetic alterations leading to the development of cancer can arise due to errors that transpire during the process of cellular division. The detrimental impact on DNA results from exposure to hazardous environmental substances, such as the chemical components found in tobacco smoke and the ultraviolet radiation emitted by the sun. Typically, the human body possesses the ability to eliminate cells that harbor DNA damage before their progression into cancerous states. However, the physiological capacity of the human body to perform such functions diminishes with advancing age. This phenomenon contributes to the increased susceptibility to cancer in older individuals [4]. Every individual's cancer exhibits a distinct amalgamation of genetic alterations. As the malignancy progresses, further alterations will manifest. Intra-tumoral heterogeneity can give rise to genetic variations among cells within a tumor [5].

1.1 Development of Cancer

A substantial portion of our present comprehension pertaining to cancer is firmly rooted in the fundamental principle characterizing it as a genetic malady, originating from a clonal population of cells that undergoes uncontrolled proliferation owing to a repertoire of acquired mutations during an individual's lifetime. These somatic mutations encompass a diverse array of genetic alterations, encompassing various types of base substitutions, deletions, insertions, and rearrangements arising from DNA breakage and aberrant rejoining, and changes in the copy number of distinct DNA segments [6]. Furthermore, it is customary for these molecular changes to encompass epigenetic modifications that exhibit stable inheritance during mitotic DNA

replication. One pertinent example of such epigenetic alterations includes changes in the methylation patterns of cytosine residues [7].

The emergence of a fully developed cancer clone within an individual is influenced by a multitude of complex interactions between environmental and lifestyle factors, alongside the interplay of genomic sequence variants that are present in the fertilized egg from which the individual embryonically develops. Crucially, these constitutional or "germline" mutations, as they are commonly denominated, have the intrinsic capacity to impact susceptibility to cancer via diverse mechanistic pathways. These mechanisms encompass not only direct perturbations to the growth of neoplastic cells but also intricate alterations to the mutation rate in non-reproductive cells and the modulation of the metabolic processes of substances that can potentially instigate cancer [8].It is widely believed that somatic mutations manifest across the genomes of all healthy cells as they undergo successive rounds of cell division during the intricate processes of prenatal development and the continual replenishment of bodily tissues throughout postnatal life [9]. However, in the context of cancer cells, their sustained and unabated division engenders an incessant accumulation of additional somatic mutations, further contributing to the molecular heterogeneity and clonal evolution characterizing the tumorigenic process [10].

Exogenous and endogenous exposures that elicit genotoxic effects on DNA can potentiate the accrual of diverse somatic mutations and elevate somatic mutation diversity. These exposures may be counteracted by proficient DNA repair mechanisms. Nevertheless, when DNA repair mechanisms prove ineffective, there exists the potential for heightened somatic mutation rates. Somatic mutations are known to exhibit a relatively stochastic distribution throughout the entirety of the genome. However, within a clonally expanding cell leading to cancer development, a specific cohort of mutations known as "driver mutations" serendipitously occur in a select set of genes referred to as "cancer genes" [11]. Consequently, these mutations disrupt the normal regulation of crucial cellular processes, such as cell growth, interactions with the surrounding tissue microenvironment, differentiation, and apoptosis, The acquisition of driver mutations confers a selective advantage to the neoplastic clone, enabling it to proliferate more aggressively than non-mutated cells derived from the same tissue. This advantageous edge facilitates the invasion of neighboring tissues and, in numerous cases, the formation of metastases [12].

The quantity of driver mutations harbored by a cancerous cell provides insight into the number of mutated cancer genes present, which in turn perturbs essential cellular processes necessary for the transformation of a healthy cell into a symptomatic cancerous clone [13]. The remaining mutations, which often constitute the majority, are commonly referred to as "passenger mutations" since they do not confer any growth advantage, as per their definition. The abundance of passenger mutations identified in a cancer genome predominantly corresponds to the cumulative count of mitotic cell divisions occurring from the fertilized egg to the cancerous cell, as well as the mutation rate associated with each of these cellular divisions. Thus, the compilation of somatic mutations within the genome of a cancerous cell signifies genetic alterations that amass over the course of multiple decades. This encompasses mutations accountable for bestowing the diverse characteristics of the neoplastic phenotype and manifests the signatures of the mutational mechanisms that initially initiated the disease [14].

1.2 Statistics of Cancer

Based on the findings of the report, there has been a significant decline of 33% in cancer mortality rates since 1991, resulting in the prevention of approximately 3.8 million deaths caused by cancer. According to the American Cancer Society (ACS) data, it is projected that in the year 2023, there will be an estimated 1,958,310 new cases of cancer and 609,820 deaths attributed to cancer in the United States [15].
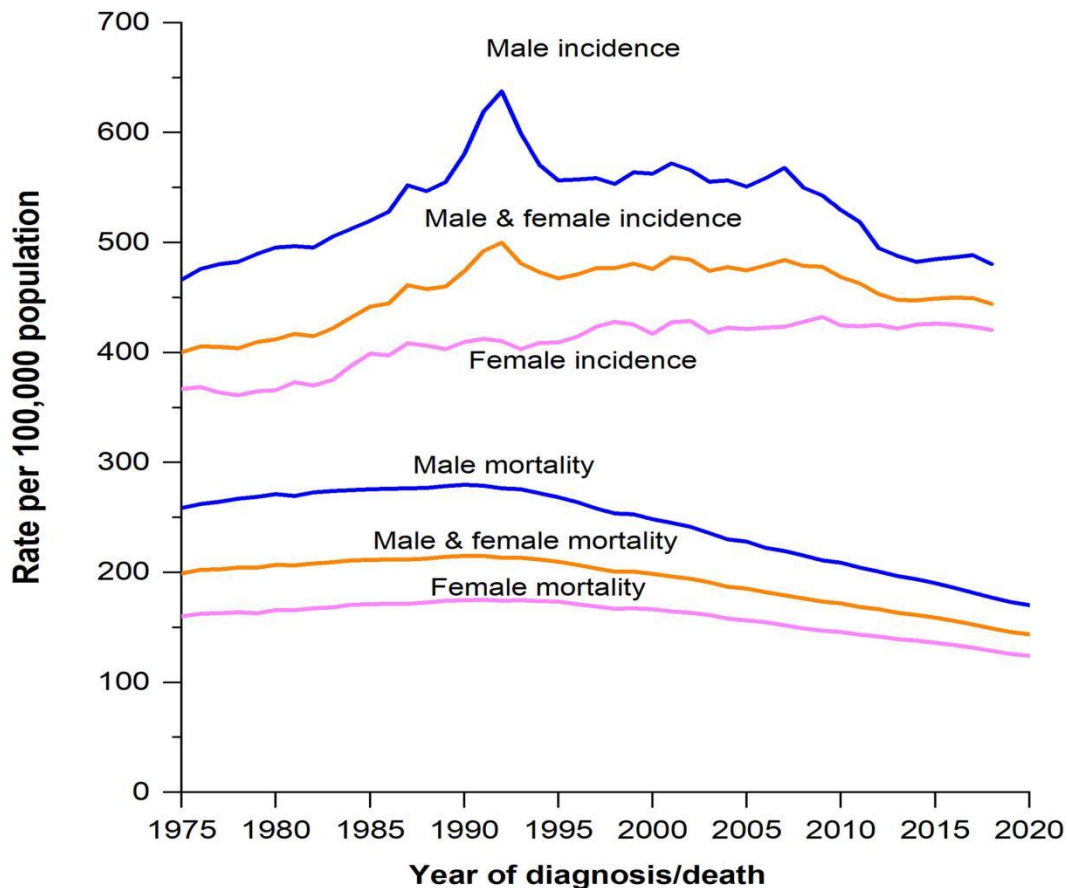
Figure 1: Cancer Statistics 2023 [15].

1.3 **Genomics of the Cancer**

An average of 33 to 66 genes in colon, breast, brain, and pancreatic solid tumors exhibit modest somatic mutations that engender modifications in their protein products. Notably, 95% of these total mutations manifest as single-nucleotide substitutions, e.g. (cytosine and guanine) C>G alterations, while the remaining mutations comprise deletions or insertion analogous to mutagens, thereby contributing to the development of these tumor forms. Remarkably, lung tumors in smokers are characterized by a substantially higher occurrence of somatic(cytosine and thyamine) CTT>CT mutations, which are base substitutions culminating in miss-sense, nonsense, and splice site alterations [16].

 Melanomas and lung tumors deviate from the norm with a striking count of ~200 non-synonymous mutations per tumor. The etiology of these mutations can be ascribed to exposure to ultraviolet light and cigarette smoke, acting as potent mutagens. Furthermore, tumors displaying DNA repair deficiencies, particularly in mismatch repair mechanisms, can accumulate a multitude of mutations

that far surpass those observed in lung or melanomas. Additionally, tumors harboring genetic changes found in the proof-reading domain of DNA polymerases POLE or POLD1 also demonstrate significant mutation rates [17].On another tangent, pediatric tumors and leukemias exhibit an average of 9.6-point mutations, suggestive of a distinct mutational landscape in these malignancies. Over time, these mutations have a pivotal function in the transition of benign. tumors into malignant counterparts, a process extensively studied in colorectal tumors [18].

The first mutation, aptly termed "gatekeeping," incites the conversion of a normal epithelial cell into a microscopic clone, effectively overriding its neighboring cells. In the context of colon tumors, the Adenomatous Polyposis coli represented as APC gene frequently houses gatekeeping mutations that culminate in the formation of tiny adenomas characterized by slow growth. Subsequently, a second mutation, often involving genes like KRAS (Kirsten rat sarcoma viral oncogene), instigates clonal development, fostering increased cell proliferation. Intriguingly, cells bearing mutations in both APC and KRAS genes are relatively rare compared to those possessing only APC mutations [19].

The emergence of mutations in genes such as TP53, PIK3CA,and SMAD4 drives clonal proliferation, propelling the progression towards malignant tumors capable of infiltrating the basement membrane and metastasizing to lymph nodes and the liver. These pivotal mutations, known as "driver," mutations, significantly aid in the development of tumor cells by conferring them with selective growth advantages, albeit at an incremental rate of 0.4% per mutation. Nevertheless, when compounded weekly, this minute growth advantage can culminate in the expansion of a billion-cell mass over the course of several years [20].

Age exhibits a noteworthy correlation with mutations in self-renewing tissue tumors, implying that more than half of the somatic mutations in these tumors occur during the pre-neoplastic phase, wherein normal cells replenish genitourinary and gastrointestinal epithelium, along with other tissues. However, these pre-neoplastic mutations are deemed "passenger" mutations, accounting for the observed discrepancy in mutation burden between a 90-year-old patient's colon tumor and an ostensibly identical tumor in a 45-year-old patient [21].Moreover, this phenomenon elucidates why advanced brain tumors and pancreatic cancers present with fewer mutations than their colorectal counterparts. The limited number of mutations in pancreatic or brain cancer precursor cells can be attributed to the fact that these tissues do not undergo the same degree of replication

as colon epithelial cells [22].Similarly, pediatric malignancies harbor fewer mutations compared to adult tumors, specifically due to the less frequent regeneration of precursor cells in children. Juvenile cancers, as well as adult leukemias and lymphomas, may necessitate fewer clonal expansion cycles than solid tumors in adults [23].

Genome sequencing studies of leukemia patients have revealed that normal precursor cells undergo random alterations prior to acquiring an initiating mutation. The occurrence of somatic mutations in tumors can be likened to an evolutionary clock, which provides valuable insights into the timing of mutational events and their implications for tumor development. Notably, the acquisition of metastatic potential in cancerous cells requires decades of cumulative mutations. Moreover, analyses of progressive colorectal and pancreatic cancer tumors have demonstrated that most mutations found in metastatic lesions are already present in the initial tumor cells [24].

Metastatic cancer progression hinges upon the precise timing of mutations, where the primary tumor may be surgically excised, but undetectable and widespread metastatic lesions persist and grow in organs like the lungs and liver [25]. Notwithstanding extensive research efforts, specific genetic mutations that distinguish metastasizing tumors from non-metastasizing malignancies have yet to be identified conclusively. Metastatic lesions have not been thoroughly investigated to unveil potential genetic abnormalities, particularly in cases where the mutations exhibit a diverse pattern. It is plausible that metastatic cancer development is governed by stochastic mechanisms alone, whereby a malignant initial tumor metastasizes over the years. The release of millions of cells daily by advanced tumors is balanced by only a small percentage of these circulating cells that manage to form metastatic lesions, a process potentially contingent upon random lodgment in a growth-friendly organ capillary bed [26]. The primary tumor's progression is primarily driven by local selection advantages rather than anticipatory future selected benefits. Compelling recent evidence of normal cells forming organoids with functional vasculature in lymph nodes bolsters the hypothesis that metastatic development may not necessarily depend on genetic changes [27].

1.4 Diagnosis of Cancer

The process of diagnosing cancer is intricate and involves a comprehensive assessment and examination conducted by healthcare professionals. When an individual exhibits symptom or possesses risk factors that elicit suspicion of cancer, medical professionals employ a variety of

approaches to attain a precise diagnosis. Various techniques can be employed, encompassing the examination of the patient's medical records, the execution of physical assessments, the implementation of imaging procedures, and the utilization of laboratory analyses, such as blood tests or biopsies [28]. The utilization of diagnostic methods by medical professionals is intended to ascertain the existence of cancer, ascertain its specific anatomical site, determine its stage and grade, and acquire essential data to inform treatment choices. The process of cancer diagnosis holds significant importance in the overall management of the disease. The utilization of personalized treatment approaches is facilitated, prognostic information is provided, emotional support is extended to patients, and contributions are made to the continuous research and advancements in the field of cancer care [29]. The attainment of optimal outcomes and enhancement of the quality of life for individuals impacted by cancer heavily rely on the prompt and precise identification of the disease. Cancer diagnosis and screening approaches include the medical history of patients, physical examination, and then diagnostic testing [30].
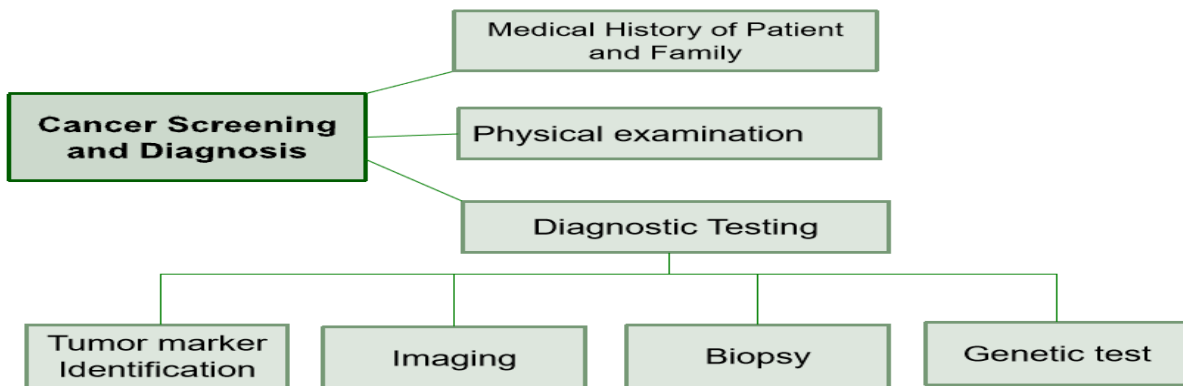
Figure 2: Cancer Diagnostic Approaches

1.4.1 Medical History and Physical Examination

The procedure of collecting medical history and conducting a physical examination involves five essential steps. Firstly, information is collected based on the specific type of tumor. Secondly, the appropriate method of diagnosis for that tumor type is determined, along with an assessment of

the progress made in the diagnostic process thus far. Thirdly, a comprehensive cancer-focused history is obtained. Fourthly, a physical examination is conducted. Finally, the collected data is organized properly to facilitate a professional presentation and ensure accurate documentation.

1.4.2 Diagnostic Testing

1.4.2.1 Tumor Markers

A tumor biomarker can be defined as a quantifiable substance or characteristic present in the human body that serves as an indicator of the existence of a tumor or imparts insights into its behavior. Biomarkers encompass a diverse range of molecules, including proteins, DNA, RNA, and distinctive cellular attributes. Tumor biomarkers are very important for diagnosing cancer, figuring out what its likely outcome will be, choosing the right treatment, and keeping track of how effectively the treatment works [31]. They can aid in the early detection of cancer since some biomarkers are raised even before the appearance of clinical signs. Furthermore, biomarkers result in the identification and division of cancer, enabling healthcare practitioners to customize treatment strategies in a precise manner. Cancer therapy efficacy and disease recurrence can be assessed through biomarker testing [32].

1.4.2.1.1 Prostate-Specific Antigen

PSA is a protein biosynthesized by both healthy and neoplastic cells within the confines of the prostate gland. The quantification of PSA concentration in the circulatory system is accomplished through the PSA test, wherein a blood specimen is dispatched to a specialized laboratory for comprehensive analysis. The test results are typically conveyed in the form of nanograms of PSA per milliliter (ng/mL) of blood [33].Healthcare professionals frequently employ the PSA test in conjunction with the digital rectal examination to elucidate the etiology of reported prostate-related symptoms in individuals [33]. Aside from prostate cancer, a diverse array of non-malignant conditions can prompt an escalation in an individual's PSA level, notably encompassing prostatitis and benign prostatic hyperplasia. While no definitive empirical evidence substantiates a causal linkage between either condition and the pathogenesis of prostate cancer, it is plausible for an individual to concurrently harbor one or both conditions and eventually manifest prostate cancer [34].

The quantitative assessment of PSA levels in the bloodstream does not adhere to a discrete normative standard distinguishing between normal and abnormal values. Historically, PSA levels below the threshold of 4.0 ng/mL were conventionally regarded as within the purview of normalcy. Nevertheless, it is imperative to recognize that certain individuals presenting with PSA levels below this established threshold of 4.0 ng/mL might indeed harbor prostate cancer, while conversely, a substantial cohort of individuals evincing PSA levels ranging from 4 to 10 ng/mL may not manifest prostate cancer [35].Moreover, multiple factors can contribute to the fluctuation of an individual's prostate-specific antigen level. Generally, lustration, it has been observed that the level of prostate-specific antigen generally exhibits an upward trend in conjunction with advancing age, the size of the prostate gland, as well as instances of inflammation or infection. The PSA level can be elevated by various factors, including recent prostate biopsy, ejaculation, or intense physical activity (such as cycling) within the 48 hours preceding the test [36]. In contrast, certain pharmaceutical substances such as finasteride and dutasteride, commonly prescribed for the management of benign prostatic hyperplasia (BPH), exhibit the capacity to reduce the PSA level. Typically, an elevated PSA level in men is positively correlated with an increased probability of prostate cancer [37].

1.4.2.1.2 Cancer Antigen 125(CA125)

Ovarian cancer ranks as the second most fatal gynecological malignancy. The biomarker CA125 has been widely utilized as the primary marker for ovarian cancer over the last forty years [38]. The utilization of CA125 as a diagnostic biomarker for the initial detection of ovarian cancer in steps I with step II has not yielded significant improvements in patients' overall survival rates. Consequently, professional societies do not recommend the utilization of CA125 screening for asymptomatic women at average risk. The dualistic model of ovarian cancer carcinogenesis posits that type II tumors are the primary contributors to the overall mortality associated with ovarian cancer [39]. Nevertheless, the occurrence of type II tumors in stages I and II is infrequent. The current emphasis on early detection of low-volume type II ovarian cancer presents a promising and significant area of interest for screening purposes. Type II ovarian cancers are typically detected at advanced stages and exhibit markedly elevated levels of CA125 compared to type I tumors. The identification of small-sized type II carcinomas in stage IIIa/b is linked to an increased probability of achieving optimal cytoreduction, which is considered the most reliable prognostic

factor for individuals diagnosed with ovarian cancer. The potential for diagnosing early sub-stages of stage III type II ovarian cancer, with the aid of CA125, may be enhanced by employing a higher cutoff point in point-of-care CA125 assays within primary care settings, as opposed to the conventional threshold of 35 U/Ml [39].

1.4.2.1.3 Carcinoembryonic Antigen

CEA is a serum biomarker that shows non-specific elevation in various malignancies, such as breast cancer, colorectal cancer, medullary thyroid cancer, and mucinous ovarian cancer. It was initially discovered in colon cancer cells by Freedman and Gold, but later found in different epithelial cells like those in the stomach, tongue, esophagus, cervix, and prostate. This glycoprotein has a molecular weight of 200 kilodaltons (kDa) and is typically produced by the embryonic endodermal epithelium during fetal development, regulated by fetal oncogenes [40]. CEA levels in the serum generally decrease after birth, but some residual amounts may be present in colon tissue. Humans have a CEA gene family with 29 genes, of which 18 are usually expressed. These genes are located close to each other on chromosome 19q13.2 [41].Due to its association with various medical conditions, elevated serum CEA levels cannot definitively indicate the specific site of cancer origin. To measure CEA, healthcare personnel or phlebotomists collect a blood sample of about 3 to 5 cubic centimeters (cc) for laboratory analysis. Potential hazards associated with the procedure are low and include needle site discomfort, stinging sensation, bruising, bleeding, or rare infections [41]. The process takes less than five minutes and does not require fasting. Sometimes, CEA testing is also done on other bodily fluids like cerebrospinal fluid, pleural fluid, and peritoneal fluid.

1.4.2.1.4 Alpha-Fetoprotein (AFP)

The serum AFP is presently utilized as a diagnostic marker for the detection of hepatocellular carcinoma). Concerning individuals with a diagnosis of chronic liver disease, it has been observed that a persistent elevation in alpha-fetoprotein levels in the bloodstream is associated with an increased likelihood of developing HCC. Consequently, the measurement of AFP levels in the blood has been employed as a means for determining a subgroup of chronic liver disease patients at a heightened risk of developing HCC. Fluctuations in AFP levels among individuals diagnosed with liver cirrhosis may serve as an indicator of the abrupt onset of viral hepatitis, the progression

of underlying liver disease, or the emergence of HCC. Additionally, it has been reported that the level of AFP exhibits interaction with certain molecular subtypes, such as EPCA positive, in cases of invasive hepatocellular carcinoma. The identification of the threshold for AFP levels is complicated by the presence of various contributing factors. When the threshold value for alpha-fetoprotein was set at 20 ng/ml, the detection exhibited a relatively favorable level of sensitivity but had a lower level of specificity [42]. Conversely, when the threshold value was increased to 200 ng/ml, the detection demonstrated a higher level of specificity but a notable decrease in sensitivity. The diagnostic staging standard for hepatocellular carcinoma in China utilized an AFP level of 400 ng/mL as the diagnostic threshold in both 2001 and 2017. Nevertheless, a meta-analysis indicates that the diagnostic efficacy of alpha-fetoprotein levels equal to or greater than 200 ng/mL might be superior. This is due, in part, to the possibility of overlooking certain early cases of hepatocellular carcinoma (HCC) in individuals with AFP concentrations ranging from 20 to 200 ng/mL if the threshold of 400 ng/mL continues to be employed as the screening criterion for HCC. Thus far, the optimal threshold of AFP for hepatocellular carcinoma (HCC) diagnosis remains a subject of controversy [43]. Furthermore, there have been reports suggesting that the combination of AFP and ultrasound detection may enhance the rate of detecting hepatocellular carcinoma. The American Association for the Study of Liver Disease and the European Association for the Study of the Liver both recommend the regular monitoring of hepatocellular carcinoma in high-risk patients through abdominal ultrasonography every six months. However, there is ongoing debate regarding the use of alpha-fetoprotein as a supplementary monitoring test, and no specific threshold for AFP has been established when combined with ultrasound for HCC monitoring [44].

1.4.2.1.5 Beta Subunit HCG

The serum test is employed as a diagnostic tool for the detection of testicular carcinoma, serving as a tumor marker. Beta-HCG levels are not typically detected in males who do not exhibit any abnormal conditions. When -HCG is found in serum, it almost often means there is cancer present. This hormone is alternatively referred to as β-HCG, beta-HCG, or beta-chain HCG. Please pay close attention to the date of the beta-HCG study. Site Specific Factor 2 should be greatest after orchiectomy and before further treatment in the collaborative stage [45]. Beta-HCG is employed as a postoperative marker to monitor the residual tumor and assess the efficacy of therapy. Patients

with testicular cancer who have had an orchiectomy will know they still have cancer that needs more care if they have beta-HCG. But when beta-HCG isn't in the serum, active cancer can't be ruled out, especially in people who have already been treated. The standard range for this measurement is 0 nm per mm [46].

1.4.2.2. Imaging

1.4.2.2.1 X-Ray

Radiography, also known as X-ray imaging, is a commonly employed technique for cancer diagnosis. X-rays, a form of electromagnetic radiation, are employed to visualize anatomical structures within the human body [47]. X-ray imaging plays a crucial role in the identification and diagnosis of malignancies, particularly those affecting the skeletal system and the thoracic region. X-ray imaging is predicated upon the principle of X-ray absorption that is specific to different types of bodily tissues. Denser tissues, such as bones, exhibit a higher capacity for X-ray absorption compared to less dense tissues, such as muscles and organs. Differential X-ray attenuations provide insights into the internal structures. The utilization of X-ray imaging for the detection and evaluation of lung cancer is prevalent [48]. Chest radiographs can identify pulmonary abnormalities, including tumors, nodules, and various lesions. X-ray imaging plays a crucial role in the diagnostic process of bone tumors. The technology can identify osteosarcoma, metastatic bone diseases, and pathological fractures. X-ray imaging is a valuable diagnostic tool for the identification and classification of bone-related malignancies, as it provides visual information regarding bone density, structural integrity, and the presence of tumors [49].

1.4.2.2.2 Computed Tomography

 Computed Tomography is a commonly employed imaging modality in the field of oncology for cancer detection and treatment. This imaging modality offers comprehensive cross-sectional representations of the human body, facilitating the observation of neoplasms, analysis of their attributes, and examination of their dissemination throughout the body [50]. CT imaging is a medical imaging technique that integrates X-ray technology with sophisticated computer processing algorithms. During a CT scan, a rotating X-ray machine captures a series of cross-sectional images, also known as slices, of the human body from various perspectives.

Subsequently, a computer is employed to reconstruct these images, resulting in the generation of intricate and 3-D depictions of internal structures [51]. CT imaging possesses a wide range of applications in the field of cancer diagnosis. The utilization of this technique is widespread in the identification, classification, and surveillance of diverse forms of malignancies, such as those affecting the lungs, liver, pancreas, and abdomen. CT scans can discern the dimensions, morphology, and positioning of tumors, while also furnishing insights into their interaction with neighboring tissues and the likelihood of metastasis to remote locations.

CT scans are commonly utilized in the diagnosis and staging of lung cancer. The ability to detect lung nodules, evaluate their dimensions and spatial arrangement, and determine the presence of lymph node engagement or distant metastasis is within their capability. CT images can additionally aid in the facilitation of biopsy procedures to acquire tissue samples to be subjected to subsequent examination [52].CT imaging provides high-resolution anatomical information, but it does entail exposure to ionizing radiation. Therefore, it is important to exercise caution to minimize unnecessary radiation dosage, especially in young patients or individuals who require frequent scans. Ongoing endeavors are being undertaken to enhance the efficiency of radiation dosage while upholding the integrity of image resolution and diagnostic precision [53].

1.4.2.2.3 Magnetic Resonance Imaging (MRI)

MRI, also called magnetic resonance imaging, magnetic resonance, and nuclear magnetic resonance imaging, helps doctors find cancer in the body and look for signs that it has spread. Magnetic resonance imaging is a valuable tool in assisting medical professionals in devising optimal treatment strategies for cancer, such as surgical interventions or radiation therapy [54, 55]. MRI is a non-invasive procedure that does not induce pain and does not require any specific preparatory measures. However, it is of utmost significance to inform both the physician and the technologist who administers the examination, about the presence of any metallic objects within the body.

The MRI scanner is a cylindrical or tubular apparatus that houses a substantial and highly potent magnet. The individual assumes a supine position on a horizontal surface that is subsequently inserted into a cylindrical structure, while the apparatus envelops the individual with a robust magnetic field. The device employs a robust magnetic field and a rapid emission of radiofrequency

waves to detect signals emanating from the nuclei of hydrogen atoms within the human body. The computer processes these signals and subsequently transforms them into a monochromatic image [55].Intravenous administration of contrast agents facilitates enhanced image clarity within the body. Upon being assimilated by the human body, the contrast agent enhances the velocity at which the tissue reacts to the magnetic and radiofrequency waves. The more powerful signals result in more distinct visual representations [56].

1.4.2.2.4 Positron emission tomography (PET)

PET imaging employs radiopharmaceuticals that are labeled with positron-emitting radioisotopes, namely 11C,18F,13N, and 15O. These radioisotopes are generated within a cyclotron. Additionally, PET imaging utilizes 82Rb and 68 Ga , which are produced through a radioisotope generator [57]. Upon the emission of a position, it undergoes annihilation upon encountering an electron nearby. This annihilation process results in the production of two annihilation photons, each possessing an energy of 511-kilo electron volts (keV). These photons subsequently propagate in opposite directions. Positron emission tomography scanners are equipped with coincidence electronics to detect pairs of photons that are detected by opposing detectors in close temporal proximity. Single unpaired photons are observed when either one of the annihilation photons is absorbed within the body or remains undetected. While the exclusion of single photons by the coincidence window is a crucial aspect, it is important to consider additional processes in PET imaging that can lead to a degradation of image contrast. These processes must be considered when performing quantitative PET imaging [58]. Therefore, it is necessary to employ a range of algorithms and techniques to address issues such as random coincidence events, scatter, dead time, and variations in sensitivity across different detectors. Attenuation correction is a crucial step in obtaining precise quantitative outcomes for PET imaging. This correction is imperative because photons emitted from the core of the entity, on average, experience a higher degree of attenuation compared to photons emitted from the outer regions. One of the benefits associated with hybrid PET/CT systems is the ability to utilize the corresponding CT images for both anatomic localization and attenuation correction [59].

1.4.2.2.5 Ultrasound

Diagnostic ultrasound is a non-invasive diagnostic modality employed to visualize internal structures within the human body. Transducers, known as ultrasound probes, generate sound waves with frequencies exceeding the human auditory threshold (above 20KHz). However, the majority of transducers currently employed operate at significantly higher frequencies, typically in the megahertz (MHz) range [60]. Many diagnostic ultrasound probes are positioned on the surface of the skin. To enhance the quality of images, it is possible to strategically position probes within the human body through various routes such as the gastrointestinal tract, vagina, or blood vessels. Furthermore, the utilization of ultrasound is occasionally employed intraoperatively through the insertion of a sterile probe into the surgical site [61].

Diagnostic ultrasound can be categorized into two main subtypes: anatomical ultrasound and functional ultrasound. The utilization of anatomical ultrasound enables the generation of visual representations of internal organs or other anatomical structures. Functional ultrasound integrates various types of data, including tissue or blood movement and velocity, tissue softness or hardness, and other physical attributes, in conjunction with anatomical images, to generate comprehensive "information maps." These cartographic representations aid medical professionals in visually perceiving alterations or variations in functionality within a specific anatomical structure or organ [62].

Ultrasound waves are generated by a transducer, which possesses the ability to both emit ultrasound waves and detect the subsequent echoes that are reflected. Piezoelectric ceramic materials, commonly referred to as piezoelectric, are frequently employed as active components in ultrasound transducers. These materials possess the capability to generate sound waves through the application of an electric field [63]. Conversely, they also exhibit the ability to generate an electric field upon being subjected to a sound wave. In the context of an ultrasound scanner, the transducer emits a focused stream of acoustic waves that penetrate the human body. The transducer receives the reflected sound waves as they encounter boundaries between different tissues along the path of the beam, such as the interface between fluid and soft tissue or between tissue and bone. When the echoes come into contact with the transducer, they produce electrical signals that subsequently generate two-dimensional images of various tissues and organs [64].

1.4.2.3 Biopsy

A biopsy is a medical procedure that is conducted to acquire a specimen of tissue or cells from a potentially anomalous region within the body, which is subsequently subjected to diagnostic assessment. The utilization of this tool is of utmost importance in the diagnosis of cancer and serves as a pivotal factor in identifying the existence, classification, and attributes of cancerous conditions. A range of biopsy techniques exists, encompassing needle biopsies, endoscopic biopsies, and surgical biopsies, which are individually designed to accommodate the distinct location and accessibility characteristics of the area under suspicion [65].

During a biopsy, a healthcare professional procures the tissue specimen while employing either local or general anesthesia, taking into consideration the intricacy of the procedure and the comfort of the patient. Subsequently, the specimen is forwarded to a pathology laboratory, wherein pathologists meticulously scrutinize it through microscopic examination and administer supplementary examinations to ascertain the existence of malignant cells, evaluate their characteristics, and ascertain the specific type and grade of cancer [66].

Biopsies are considered to be of significant value in the realm of cancer diagnosis due to their ability to offer direct access to the affected tissue, thereby facilitating accurate determination of the presence and nature of the disease. This facilitates healthcare professionals in making well-informed decisions regarding treatment alternatives, including surgical interventions, chemotherapy, radiation therapy, or targeted therapies [67]. Furthermore, the utilization of biopsies plays a crucial role in the process of cancer staging, as it enables the evaluation of the degree of tumor dissemination and the detection of any indications of cancerous presence in adjacent lymph nodes or other surrounding tissues [68].

1.4.2.3.1   Needle Biopsy

Needle biopsy is a general term that's often used to describe inserting a special needle through the skin to collect cells from a suspicious area. Doctors call this a percutaneous tissue biopsy. A needle biopsy is often used on suspicious areas that healthcare providers can feel through the patient's skin, such as breast lumps and enlarged lymph nodes. When combined with an imaging procedure, a needle biopsy can be used to collect cells from an area that can't be felt through the skin [69].

1.4.2.3.2 Endoscopy

During an endoscopy procedure, a medical professional uses a thin and flexible tube called an endoscope with an illuminating mechanism at its tip to visually examine internal anatomical structures in the human body [70]. To perform analysis, specialized instruments are inserted through the tube to extract a small tissue sample. The choice of a specific endoscopic biopsy procedure depends on the location of the area of concern. Endoscopes can be introduced through the oral cavity, rectum, urinary tract, or a minor surgical opening in the skin. Different endoscopic biopsy techniques include cystoscopy for retrieving bladder tissue, bronchoscopy for acquiring lung tissue, and colonoscopy for collecting colon tissue. Depending on the procedure, a sedative or anesthetic may be administered beforehand [71].

1.4.2.3.3 Bone Marrow Biopsy

A bone marrow biopsy may be recommended by healthcare providers when abnormal blood test results are observed or when there is suspicion of cancer affecting the bone marrow. Bone marrow is a porous substance found within larger bones where hematopoiesis takes place, leading to the production of blood cells. This procedure is commonly used for diagnosing various hematological disorders, both malignant and non-malignant. It can provide valuable insights into the underlying causes of these conditions [72].

 The bone marrow biopsy is particularly useful for diagnosing hematologic malignancies such as leukemia, lymphoma, and multiple myeloma. During the procedure, a healthcare provider extracts a sample of bone marrow from the back of the hipbone using a long needle. In some cases, the sample may be taken from other skeletal structures in the body. To ensure patient comfort, a local anesthetic or other medications may be administered during the procedure [73].

1.4.2.3.4 Surgical Biopsy

In cases where conventional biopsy methods are unable to access the target cells or have produced inconclusive results, a healthcare provider might recommend a surgical biopsy. This procedure involves a surgeon making an incision on the patient's skin to gain access to the suspicious area of cells. Various surgical biopsy techniques exist, such as removing a breast lump to investigate potential breast cancer or extracting a lymph node to assess the possibility of lymphoma [74].

Surgical biopsy procedures aim to excise a portion of a potentially malignant cell cluster, although sometimes the entire affected area may be removed. Local anesthetics are commonly used to numb the biopsy site, while certain cases may require general anesthesia to render the patient unconscious during the procedure. In some instances, hospitalization might be necessary following the biopsy [75].

1.5 Biosensors

Ultrasensitive biosensors are revolutionizing personalized medicine by tailoring diagnostic approaches to individual patients' unique biochemistry. These biosensors must meet certain criteria: they should be sensitive to detect clinically relevant biomarker concentrations in biological samples and selective, requiring suitable biological recognition elements [76].

Graphene-based electronic biosensors have gained significant attention since the Manchester group's discovery of the electric field effect in graphene in 2004. These sensors operate by detecting changes in the electrical conductance of the graphene channel when molecules are adsorbed onto its surface. Graphene's unique surface composition, with all carbon atoms situated on the outermost layer, makes it highly receptive to changes in its surroundings, potentially enhancing its sensitivity [77].

Graphene possesses exceptional electrical properties such as high mobility and low intrinsic electrical noise, resulting in enhanced sensitivity compared to conventional bioassays. Its ideal crystal lattice lacks dangling bonds, making it chemically inert, which has motivated efforts to interface graphene with targeted recognition elements. Various biochemical molecules and chemical treatments, both covalent and non-covalent, have been explored for this purpose [78].

1.5.1 Graphene Field Effect Transistors

Graphene nano-electronics provides a versatile framework for a wide range of biochemical sensing applications, particularly in the field of cancer detection. Various mechanisms, such as charge transfer, charge scattering, capacitive effect, and field effect, can be used for detection. The field effect, which refers to the change in a material's electrical conductivity under the influence of an external electric field (e.g., induced by a charged biomolecule), is widely recognized as the most reliable sensing mechanism. This has led to the development of the graphene field-effect transistor

(GFET), which has sparked significant research in using GFETs for label-free chemical and biological sensing applications [79].

GFETs have been explored for detecting specific cancer biomarkers, such as circulating tumor cells, proteins, nucleic acids, or other molecules that indicate the presence or progression of cancer. The surface of the GFET is modified with antibodies or aptamers that selectively bind to these biomarkers. When biomarkers bind to the functionalized GFET surface, it alters the electrical conductivity of the graphene layer, generating a detectable electrical signal [80].One major advantage of GFET-based biosensors is their ability to detect and quantify biomarkers without the need for additional labels or tags. This label-free approach streamlines the detection process, reduces costs, and minimizes potential inaccuracies or perturbations of biomarkers' behavior.

The unique electrical properties of graphene make GFETs highly sensitive to minute changes in their surroundings. This high sensitivity allows GFETs to detect even low concentrations of biomarkers, enabling early detection and continuous monitoring of disease progression. This heightened sensitivity ensures accurate identification of cancer biomarkers, leading to reliable diagnostic data. Graphene-based biosensors, like GFETs, can be scaled down and integrated into portable devices, making them suitable for point-of-care diagnostic applications. These devices can be used in resource-limited or geographically isolated regions, improving access to cancer diagnostics and early intervention. GFET biosensors offer enhanced portability and user-friendliness, decentralizing diagnostic procedures and bringing cancer detection closer to the patient. This advancement enhances patient convenience and treatment outcomes. Harnessing graphene's exceptional properties holds great promise for the development of GFET-based biosensors, contributing significantly to cancer diagnostics. Further research and development can improve the sensitivity, specificity, and versatility of GFET-based biosensors, leading to enhanced cancer detection, personalized treatment approaches, and ultimately, improved patient care. treatment approaches, and ultimately, improved patient care [82].

1.6   Research Problem

It is estimated that about half of the global population will face a cancer diagnosis at some point in their lives, making cancer the second leading cause of death worldwide. The majority of cancer-related deaths occur in low to middle-income countries, adding to the burden of this disease, which

amounts to a staggering $1.16 trillion annually [83]. Detecting cancer at an early stage is crucial for successful treatment and reducing mortality rates.

Currently, medical professionals rely on various imaging techniques and the analysis of tissue morphology (histopathology) or cellular characteristics (cytology) to identify cancer in a timely manner. However, these imaging modalities, such as X-ray, MRI, CT, endoscopy, and ultrasound, can only detect cancer when there are visible tissue abnormalities. Unfortunately, they cannot distinguish between benign and malignant lesions [84].Radioimmunoassay (RIA) is commonly used in laboratory settings for cancer diagnosis. However, during this phase, cancer cells may have already proliferated and spread to other parts of the body, a process known as metastasis. Therefore, RIA may not be sufficient for early cancer detection [85].

While cytology and histopathology are also used as standalone methods for early cancer detection, they have limitations in their effectiveness. As a result, the development of technologies specifically targeted at detecting cancer at its early stages, before metastasis occurs, remains a significant challenge [86]. In summary, early detection of cancer is crucial for improving treatment outcomes and reducing mortality rates, especially in countries with limited resources. Advancements in technology are needed to enhance early-stage cancer detection and differentiate between benign and malignant lesions more effectively.

1.7 Study Objectives

- Development of a single blood test for the diagnosis of multiple types of cancer.
- A simple common biomarker based on epigenetic changes will help in the early detection of cancer.
- Early diagnosis will improve the treatment and increase cancer survival.
- Establishment of linkage between academia, healthcare industry, and diagnostic
- Highly sensitive will provide instantaneous measurement using a small amount of analyte.
- Improvement of GDP growth by decreasing imports and increasing export.

1.8   Significance of Research

The significance of our study is to identify new biomarkers and devise novel screening techniques to improve the early detection of cancer. The identification of distinct biomarkers that are indicative of cancer in its early stages facilitates the development of diagnostic tests with heightened sensitivity and specificity. Consequently, these tests enable the detection of cancer before the manifestation of observable symptoms. In addition, the advancement of non-invasive or minimally invasive screening techniques may catalyze increased participation in routine screenings, thereby facilitating the detection of cancer during its initial phases. This initiative equips healthcare professionals with the necessary resources and expertise to successfully implement screening programs, develop innovative diagnostic techniques, and deliver timely interventions. As a result, patient outcomes are enhanced, and the overall impact of cancer on individuals and society is diminished.

Chapter 2: Literature Review

Exosomes play a critical and pivotal role in mediating intercellular communication, exerting their profound influence on various physiological and pathological processes, particularly in the context of cancer patients. They accomplish this by efficiently transmitting a diverse array of messages. Notably, circular RNAs (circRNAs) encapsulated within exosomes have recently emerged as crucial regulators of numerous pathological pathways, and there is mounting evidence supporting their significance. These exosomal circRNAs, originating from donor cells, orchestrate intricate crosstalk with recipient cells, either locally or distantly, thereby fostering the progression and dissemination of cancer. Their indispensable roles extend to shaping the tumor microenvironment (TME) by influencing crucial aspects such as tumor immunity, metabolic processes, angiogenesis, drug resistance, epithelial-mesenchymal transition (EMT), invasion, and metastasis. Essentially, exosomal circRNAs exert multifaceted impacts, effectively modulating the fundamental hallmarks of cancer, with a primary focus on the hallmark traits within the tumor microenvironment. The considerable potential of exosomal circRNAs in cancer diagnosis and treatment holds the promise of bridging the gap between fundamental research and tangible clinical applications [87].

The present study revolves around state-of-the-art advancements in the domain of label-free chemical vapor deposition (CVD) graphene field effect transistor (GFET) immunosensors, meticulously designed for the sensitive and precise detection of Human Chorionic Gonadotropin (hCG), a glycoprotein biomarker associated with specific cancer types. The intricacies of fabricating these GFET sensors involve a strategic implementation of photolithography techniques on a Si/SiO2 substrate, complemented by the application of evaporated chromium and sputtered gold contacts. To achieve functional specificity, the channels of graphene field-effect transistors (GFETs) are astutely modulated through the attachment of a linker molecule, thereby facilitating the effective immobilization of anti-human chorionic gonadotropin (hCG) antibodies on the graphene surface. The experimental findings gleaned from studying the interaction between the antibodies and varying concentrations of the hCG antigen have furnished invaluable insights into the unparalleled detection limits of the GFET sensors. Employing the four-probe electrical measurement technique, the sensors have unequivocally demonstrated their capability to detect astonishingly low hCG concentrations, surpassing even 1 pg/mL. Moreover, the investigation has unveiled the substantial impact of annealing on significantly enhancing the carrier transport

characteristics of graphene field-effect transistors (GFETs). The annealing process induces a shift in the Dirac point, also known as the Fermi level, while concurrently reducing p-doping when utilizing a back-gate configuration. The versatile nature of the developed GFET biosensors holds vast applicability in a wide array of medical diagnostic applications, extending beyond cancer research to encompass diverse areas such as neurodegenerative disorders, including Alzheimer's and Parkinson's, as well as cardiovascular disorders.

In a separate and distinct study, LG-GFET biosensors have been ingeniously harnessed for the detection of exosomes. Leveraging the intrinsic conductivity modulation of LG-GFETs, attributed to the negatively charged and n-type doped graphene reacting to exosome concentration, the drain-source current fluctuations in LG-GFETs offer an inherently discriminating measure for precisely assessing exosome concentration. Comparative analyses, meticulously pitting exosome-free blank groups against those containing exosomes, have revealed an impressively high degree of change in the Dirac-point gate voltage (V CNP) using static methodology and saturation I ds (drain-source current) via a dynamic approach, with increments surpassing a remarkable 80% and 18.8%, respectively. The rate of change in V CNP and saturation I ds, relative to exosome concentrations, is equally noteworthy, exceeding 7% and 12.5%, respectively. Notably, dynamic LG-GFET biosensors enable the rapid detection of exosome concentrations within an incredibly short span of merely 30 seconds, thus underscoring their immense potential for efficient and accurate clinical use in medical diagnoses [88].

Meanwhile, within the context of the formidable global health threat posed by the SARS-CoV-2 virus-caused COVID-19, the demand for early diagnosis and management assumes paramount importance. In this context, the study explores the ingenious utilization of Graphene-based Field-Effect Transistor (Gr-FET) to rapidly and with remarkable sensitivity detect the presence of the SARS-CoV-2 Spike S1 antigen (S1-Ag). Facilitated by carbodiimide chemistry, the in-house developed anti-spike S1 antibody (S1-Ab) is judiciously immobilized on a carboxy functionalized graphene channel. An exhaustive array of sophisticated spectroscopic, microscopic, and stability studies, such as Ultraviolet-visible spectroscopy, Fourier-Transform Infrared Spectroscopy, X-ray Photoelectron Spectroscopy (XPS), Atomic Force Microscopy (AFM), Optical Microscopy, Raman Spectroscopy, and Scanning Electron Microscopy (SEM), in conjunction with ELISA and device stability investigations, are deftly harnessed to meticulously characterize the Gr-FET

bioconjugation and fabrication process. Real-time monitoring of Ag–Ab interaction resistance changes effectively and accurately evaluates the electrical response of the device. Notably, the Gr-FET devices exhibit impressive sensitivity and specificity, demonstrating the capacity to detect minute S1-Ag concentrations spanning an extensive range from 1 fM to 1 μM, with an extraordinary limit of detection as low as 10 fM in standard buffer. Therefore, these S1-Ag-detecting devices offer a potent and powerful tool in the relentless fight against COVID-19, enabling sensitive and specific detection even at extraordinarily low levels [89].

In the context of nephrogenic diabetes insipidus (NDI), wherein the kidney's impaired response to anti-diuretic hormone (ADH) results in increased urine loss, the restoration of water equilibrium in an artificial kidney represents a paramount challenge. Addressing this challenge in a pioneering manner involves the direct immobilization of an ADH-specific aptamer on a surface-modified suspended graphene channel, ultimately giving rise to an ultrasensitive and highly selective aptameric graphene-based field-effect transistor (GFET) sensor for ADH detection. Emulating collecting tube receptors, the aptamer directly probes the ADH peptide at the sensing location, eliciting a profound modification in the graphene channel's charge carrier concentration. The ADH biosensor has exhibited unprecedented sensitivity, detecting ADH concentrations spanning from astonishingly low levels of 10 ag/mL to 1 pg/mL, resulting in a substantial relative change of current ratio from 5.76 to 22.60. Impressively, the ADH biosensor boasts an unparalleled detection limit as low as 3.55 ag/L and demonstrates a remarkable sensitivity of 50.00 μA·(g/mL) −1. In specificity studies, the ADH biosensor has unequivocally proven its exceptional selectivity by showcasing a significantly higher current value compared to other biomolecules, registering an impressive 338.64 μA in PBS and an equally notable 557.89 in human serum. These experimental findings eloquently demonstrate the extraordinary ultrasensitivity and selectivity of the ADH biosensor for precise ADH detection in both PBS buffer and ADH-spiked human serum [90].

Chapter 3: Methodology
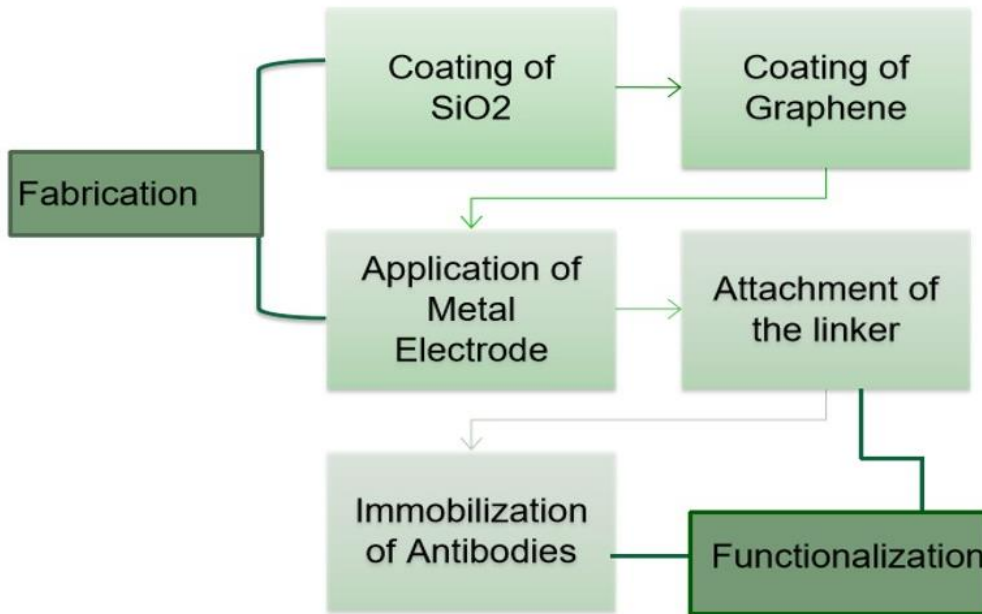
Figure 3: Key Steps of Methodology

3.1 Fabrication of Device

3.1.1 Cutting of Silicon Rubber

4×4mm silicon rubber sheets were cut with the help of a laser cutter at power 100. Silicon adhesives sheets of 4×4mm were also cut with the help of a laser at the power of 50. The purpose of using a laser cutter was to attain the exact dimensions for the sensor. Initially, the dimensions were 15×15mm but then optimized to 4×4mm to attain better results.

3.1.2   Application of silicon adhesive on silicon rubber

As silicon rubber is hydrophobic, the coating was hydrophilic therefore it was made hydrophilic by applying silicon adhesives. Silicon adhesive sheets were applied with the help of manual force. rubber substrate.

3.1.3 Preparation of 60% PVP

60% PVP was prepared by adding slowly 60 grams of PVP in 100ml of distilled water and mixing with the help of a magnetic stirrer for 2-3 hours at 60℃ until a homogeneous solution was formed. Slow addition of PVP is necessary to avoid clamp formation. The stock solution was kept at room temperature for further use in experiments.

3.1.4 Preparation of SiO2 Solution

The SiO2 solution was formed; with the volume ratio 3:2:4 TEOS (tetra ethyl orthosilicate), ethanol, and distilled water were intermixed with a magnetic stirrer for 30min at 27℃.150 microliter of HCL was put into formulating the solution for dilution and then kept at 27℃ for 24 hours. Then, it is called SiO2-Sol. The pH of the solution was measured, slightly acid 6.

3.1.5 Preparation of SiO2 -PVP Solution

SiO2-PVP solution was formed initially at 3 different ratios.

- SiO2: PVP   90:10
- SiO2: PVP   80:20
- SiO2: PVP   70:30

1 ml of 60% PVP was mixed in 5 ml of distilled water for 15 min at 50℃. After that 9ml 0f SiO2-sol were taken and mixed slowly into the PVP solution for 30min at 50℃. The same procedure is repeated for all the ratios. For 80:20, 8ml SiO2 were added in 2ml of PVP While for 70:30, 7ml of SiO2 were mixed 3ml 0f 60%PVP.

3.1.6 SiO2 Coating

The solution was then coated on silicon Adhesive by doctor blading. The half of samples were left overnight to dry in an open-air atmosphere and half were kept in a laboratory oven at 70℃ overnight to dry at elevated temperatures.

3.1.7 Conductance Measurements

After drying the sample, the conductive or non-conductive nature of the coatings was measured with the help of a simple DMM meter. The two electrodes of the DMM meter were kept at both edges of the coating. The value of resistance was measured to check the conductive nature of the

coating. The two leads attached to the electrode were connected to the opposite face in the DMM meter.

3.1.8   Optical Profilometry

The roughness, height, intensity, and thickness profile of the SiO2 coating were measured with the help of a 2D Non-Contact Profilometer, PS-50, NANOVEA, USA. For obtaining the exact thickness values some portion at the edges of the substrate left non-coated to compare the height profile before and after coating.

3.1.9 Dielectric Measurements

Dielectric constant measurement was performed with the help of BI-870. The silicon substrate with SiO2 coating of $1*1cm^2$ area and 3.5 mm thickness were prepared for the analysis. The two ratios of SiO2 and PVP were used.

3.1.10 Preparation of 1%CMC

1% Carboxymethyl cellulose was prepared by adding slowly 1gram of CMC in 100ml of the distilled water and mixing with the help of a magnetic stirrer for 1-2 hours at 50 Č. The stock solution was kept at room temperature for further use in experiments.

3.1.11 Preparation of Graphene Solution

Different quantities of graphene and CMC were prepared.

- 500 mg of graphene in 5ml of 1% CMC
- 500mg 0f graphene in 4ml of 1%CMC
- 500mg of graphene in 3ml of 1% CMC

500 mg of graphene was mixed in 5 ml of 1% CMC with the help of a magnetic stirrer for 1 hour at 50℃ degrees in a 50 ml beaker. The beaker was covered with aluminum foil to avoid the evaporation of water that CMC contained. The above procedure was repeated for 4ml and 3ml of CMC.

3.1.12 Graphene Coating

To attain the graphene coating the above solutions were coated on already SiO2-coated silicon rubbers. The coating was done by a doctor blading. Half of the coated samples were kept bear in

Petri plates in Oven at 70℃ while the other half were kept in Petri plates covered with aluminum foil.

3.1.13 Optical Profilometry

For the measurement of the thickness of the coating of graphene, some portions of a substrate coated with SiO2 coating were left non-coated to compare the height profile.

3.1.14 Conductance Measurements

After drying the specimen, the non-conductive or conductive behavior of the coatings was measured by a simple DMM meter. The two electrodes of the meter were kept at both ends of the coating. The value of resistance was measured to check the behavior of the coating.

3.1.15 Mechanical Strength Measurement

Mechanical strength of the sample after Sio2 Coating and after graphene coating on SiO2coating was measured with the help of the ASTM D638. The sample for measurements was of length greater than 28mm, width of 8mm, and thickness of 1mm. ASTM D638 was conducted using a tensile force on both samples; different mechanical properties of the material were measured under stress. The machine was a universal testing machine also known as a tensile testing machine. For the strength measurement, the tensile rate ranged from 1 to 500mm/min or 83.35 micros per second.

3.1.16 Surface Analysis

Surface analysis was performed after both coatings with the DSX1000 Digital Microscope.DSX incorporates the quality of optical technologies with the ease of use of digital technologies. The DSX1000 digital microscope was used to observe and measure the surface properties e.g. roughness and thickness of the coatings, until the coating showed cracks.

3.2 Functionalization

3.2.2 Preparation of PBS Solution

The PBS buffer solution was prepared by mixing one PBS tablet in 100ml of deionized water and a stirrer for half an hour at room temperature. The resulting solution was 1X PBS buffer.

3.2.3 Linker Attachment

Linker solution was prepared by adding 1.9270mg of linker in 5ml of 1:3 v/v solvent dimethylformamide: methanol. The device was functionalized by pipetting 50 microliter of the linker solution onto the sensor, in such a way that it should cover the electrodes as well. The sensor was covered and incubated in the vacuum desiccator to avoid evaporation for 2 hours at room temperature. After 2 hours of incubation, sensors were washed in methanol and dried in liquid nitrogen for a few seconds.

3.2.4 Antibody Immobilization

20 microliters of antibody were taken and diluted in 1X PBS buffer. Then 5ml from the stock solution was taken and diluted further in 1ml, the same as with the 10ml. Then 20 microliters of antibodies from stock, 10ml, and 5ml solution were pipetted on the sensor in such a way that it should cover the working electrodes as well. The sensors were incubated at 2-8℃ for 4hrs to 6 hrs at 20rpm. After that, the sensors were washed in 1X PBS and dry in liquid nitrogen for a few seconds.

3.2.5 Blocking of the Antibodies

PBST was prepared by adding 0.05ml of Tween-20 (0.05%) to 100ml of PBS. 1% non-fat milk was prepared by adding 1 gram of non-fat in 99ml of PBST and mixing thoroughly for 3-4 hours at room temperature followed by incubation at 2-8℃ for 4-6 hours. 50 microliter of PBST containing 1% non-fat milk to the working electrode and then incubated at 2-8℃ at 20 rpm for 4 hours. Washing was performed with deionized water and then rinsed with PBST and then followed by drying in liquid nitrogen.

3.2.6 Surface Analysis

Surface analysis was performed by 1000X digital microscopy for only graphene coating, after the attachment of the linker to the sensor, and after the immobilization of antibodies on the surface of the sensor. The roughness and height profile were measured.

3.2.7 Scanning Electron Microscopy

Scanning electron analysis was performed on a 4×4mm sample. The sample was first kept in an oven to remove the moisture then coated with gold. Analysis was performed on three samples, one

with graphene only, the second one has a linker and the third has graphene, a linker, and the antibody. The analysis was performed in a vacuum environment and at different magnifications.

3.2.8 Fourier Transform Infrared Analysis

Fourier Transform Infrared Spectroscopy was performed to analyze the functional groups present in our samples .Three samples were prepared one was graphene, the second one contained a linker and the third one had both linker, graphene, and antibody. The transmittance was measured against the wavelength range of 400-4000.

3.2.9 X-Ray Diffraction

Crystalline structure, phase composition, and orientation were measured by a non-destructive method, known as the X-ray diffraction method. Every compound has a different angle of diffraction due to the unique properties that it possesses. The angle of diffraction range sets from 0 to 100 while the intensity range was up to 1000. The samples were prepared, graphene, with linker and third linker antibody and graphene.

3.2.10 UV Analysis

The absorbance of different components in our three solutions was measured to confirm their presence. UV absorbance was measured in a micro-plate reader having a wavelength range from 0 to 400. Three samples were the same as those prepared above. UV samples were in solution form.

3.2.10 Current- Voltage Measurements

Linear sweep voltammetry was performed to measure the current in response in the patient and the control. Two surface electrodes were connected to the silver electrodes present at both edges of the sensor. The third electrode was grounded. The blood sample and plasma were pipetted on a working electrode to measure the current response. The blood sample was from a uterine cancer patient.

Chapter 4: Results and Analysis

4.1 Fabrication

SiO2 coating, graphene coating and the application of electrode were included in the fabrication portion of the device. Optical profilometry, surface analysis, dielectric and conductance measurement were performed for the characterization purpose.

4.1.1 Optical Profilometry

Optical Profilometry was being performed for the roughness, thickness, and height analysis of the SiO2 coating and graphene coating.

4.1.1.1 SiO2 Coating

The above results show that by varying the concentration of SiO2 and PVP the roughness height and thickness profiles are also affected. The desired thickness was obtained at 90:10 of PVP and SiO2, T that was 4.76 micrometers, and roughness was also below 250 micrometers.

Table 1: Optical Profilometry of SiO2 Coating

Sample	Composition	Substrate	Maximum Height (μm)	Mean Height (μm)	Width (mm)	Rt (μm)
1	95:5 PVP:SiO2	Silicon Rubber	92.3	4.62	4.97	307
2	90:10 PVP:SiO2	Silicon Rubber	55	4.76	5.88	143
3	80:20 PVP:SiO2	Silicon Rubber	143	25.6	2.98	122

4.1.1.2 Graphene Coating

The individual profilometry of graphene was also performed the mean height measured was 25.6 micrometers while the roughness was 122 micrometers as shown in the table 2 below.. All the parameters were increased when two coatings were combined. The height reached 40.11 and the roughness increased up to 357micrometers. Results indicate that the coating of two materials was successfully done.

Table 2 : Optical Profilometry of Graphene Coating

Sample	Composition	Substrate	Maximum Height (μm)	Mean Height (μm)	Width (mm)	Rt (μm)
1	• 4ml CMC • 500mg Graphene	Silicon Rubber	143	25.6	2.93	122
2	• Graphene • SiO2	SiO2 Coating	200	40.11	2.98	357

4.1.2 Surface Analysis

Morphology of the surface after and before both SiO2 and graphene coating was performed by microscope with magnification 1000X.

4.1.2.1 SiO2 Coating

This represents the 1000x microscopic image of the substrate after the coating of SiO2. This indicates that SiO2 was successfully coated because the roughness and height profile changed after the coating.

Figure 4: Microscopic Images of SiO2 Coating

4.1.2.2 Graphene Coating

Figure 5 below represented the morphology of graphene coating on SiO2 coating. Roughness and height were increased indicating that graphene was coated.
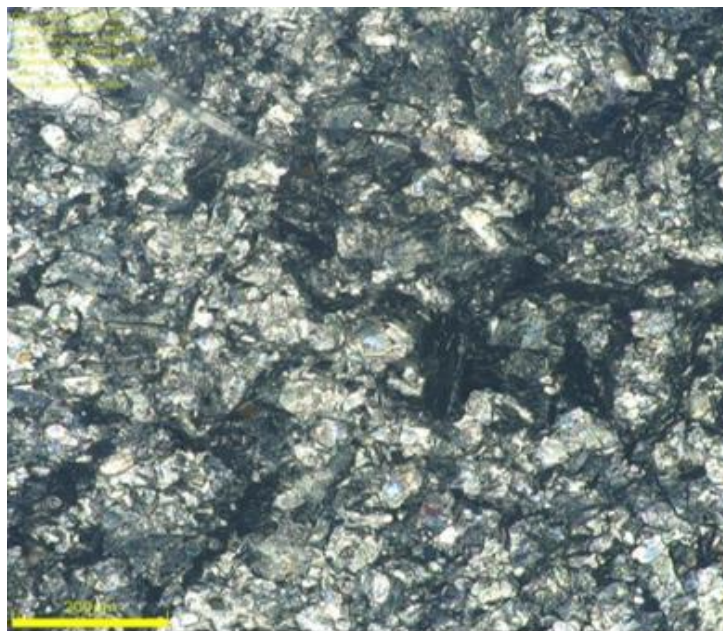
Figure 5: Microscopic Image of Graphene Coating

4.1.3 Dielectric Measurements

The dielectric constant was measured as shown below. Sample A contained the PVP: SiO2 in a 20:80 composition while sample B contained SiO2: PVP IN a 90:10 ratio. The dielectric constant of SiO2 IS 3.9 but it decreases by the addition of the binder. In sample one it was 2.4 but it increased up to 2.5 in sample B as the concentration of binder was decreased in sample B.
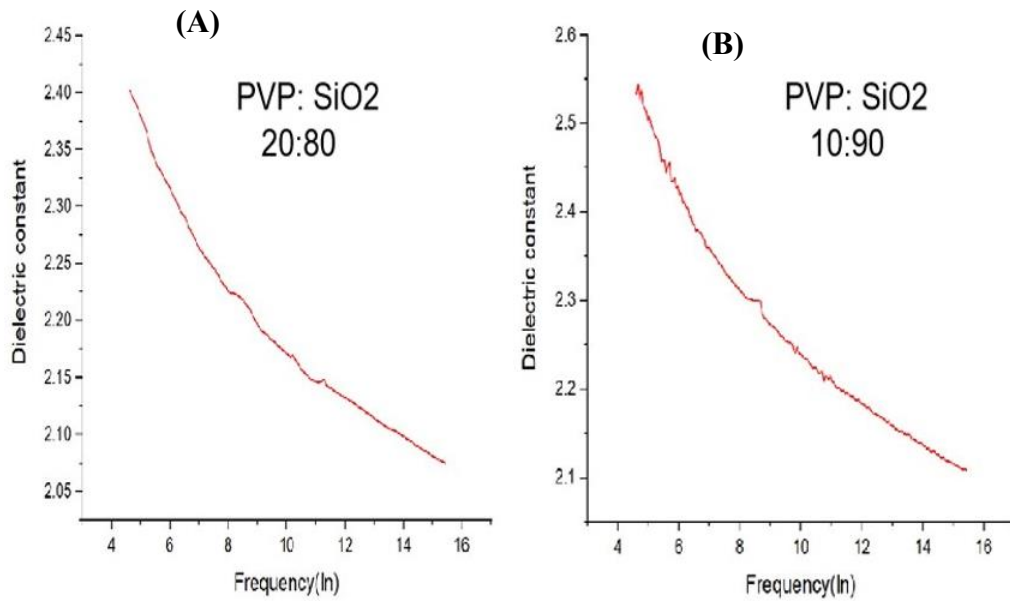
Figure 6: Dielectric Measurements (A)&(B)

4.1.4 Conductance Measurements

DMM was used to analyzed the electrical properties of the specimen before and after SiO2 coating and graphene coating. Analysis was being done on the basis of resistance measurements.

4.1.4.1 SiO2 Coating

The SiO2 coating Showed an open loop when two electrodes were placed at both edges of the coating. Open loop presence indicated that the coatings were non-conductive. That is a good property because we used SiO2 as an insulating layer.

Table 3 : Conductance Measurement of SiO2 Coating

| Sample	Composition	Resistance Before(Ω)	Resistance After(Ω)	Interpretation
1	20:80 pvp:SiO2	O.L	O.L	Non- Conductive
2	10:90 PvP:SiO2	O.L	O.L	Non-Conductive

4.1.4.2 Graphene Coating

The substrate was non-conductive as showed the open loop in the DMM meter, but the Graphene Coating resistance above 170 ohm was observed that indicated that graphene coating was conductive, and a circuit could be formed.

Table 4: Conductance Measurement of Graphene Coating

Sample	Composition	Resistance Before(Ω)	Resistance After(Ω)	Interpretation
1	• 4ml CMC • 500mg graphene	O.L	176	Conductance
2	• 4ml CMC • 500mg graphene	O.L	170	Conductance

4.1.5 Mechanical Strength Analysis

There was a significant increase in the mechanical strength after the coating of graphene. Moreover, graphs also show the elastic behavior of the coating, as indicated in the figure 7 below.
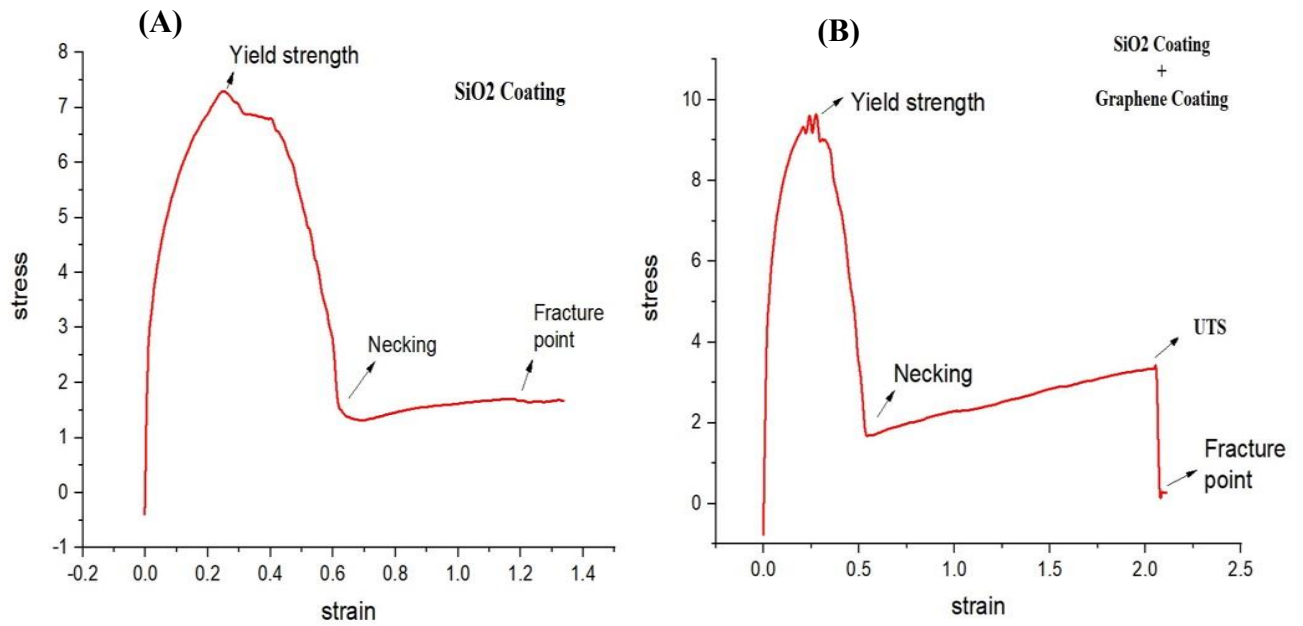
Figure 7: Mechanical Strength Measurement (A)&(B)

4.2 Functionalization

Funtionalization comprises the attachment of the linker to the device and then immobilization of antibodies on sensor through linker. Surface Analysis, SEM, FTIR, XRD and IV was performed.

4.2.1 Surface Analysis

Figure 8 below is indicating that there was no presence of a white particle in the graphene, White particles showed in the linker-based sample while in the antibody sample, yellow-colored bodies type structure appeared that confirms that our antibodies were successfully linked to the graphene via a linker. There was also a change in the height and roughness of the linker and antibody-based sample. The change confirmed the presence of the antibody as height and roughness were increased.
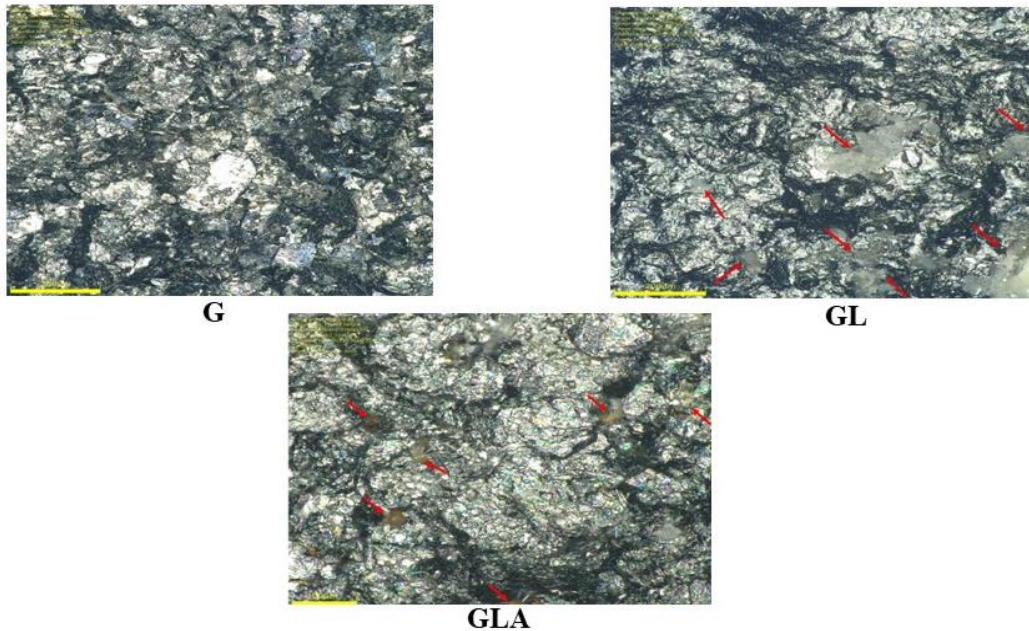
Figure 8: Surface Analysis (A) Graphene (B) Linker (C) Graphene Linked Antibody

4.2.2   Scanning Electron Microscopic Analysis

Images of scanning electrons below showed that there was no inking substance in a sample containing graphene, while white linking substances appeared in a linker sample. Figure GLA represented the presence of antibodies because the white substance was shown to be immobilized on graphene via a linker.
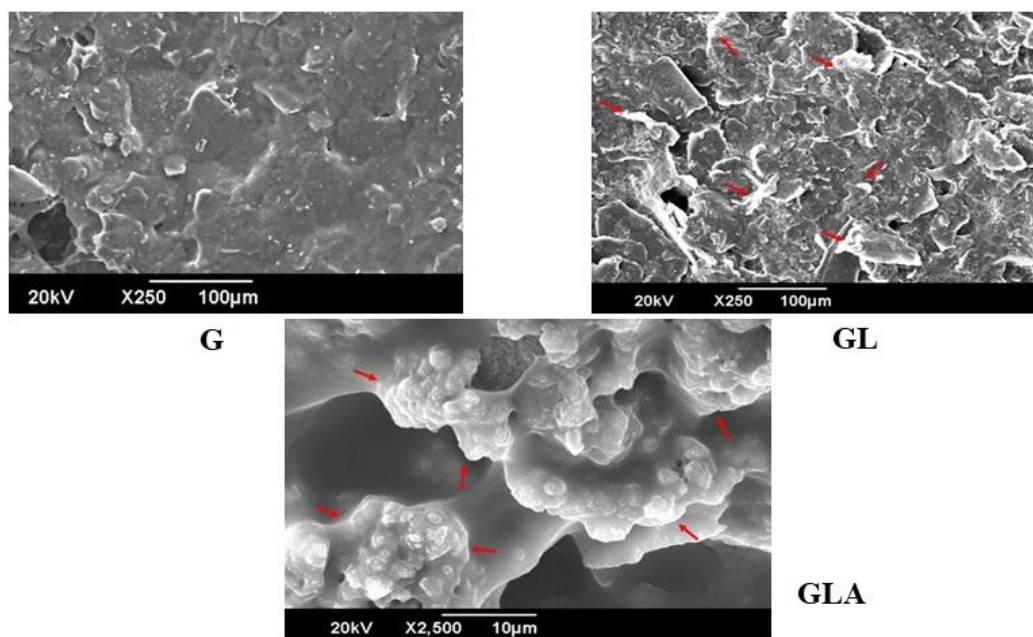
Figure 9: SEM Analysis: (A) Graphene (B) linker (C) GLA

4.2.3 FTIR Analysis

Transmittance was measured because our sensor-coated side was functionalized only. The wavelength range was from 500 to 4000. Transmittance scale up to 100. There was the presence of C=C at 2170 fig(a) that confirmed the presence of the graphene, the peak at the value 2973 in fig(b) showed the presence of ester our linker was ester in nature. Peaks at 3354 showed the presence of the NH2 group while at 2852 showed COOH, the presence of these two groups in addition to the groups of c=c and ester gave assurance of successful immobilization of antibodies on the sensor. Because all three groups shown in the sensor functionalized with the antibodies
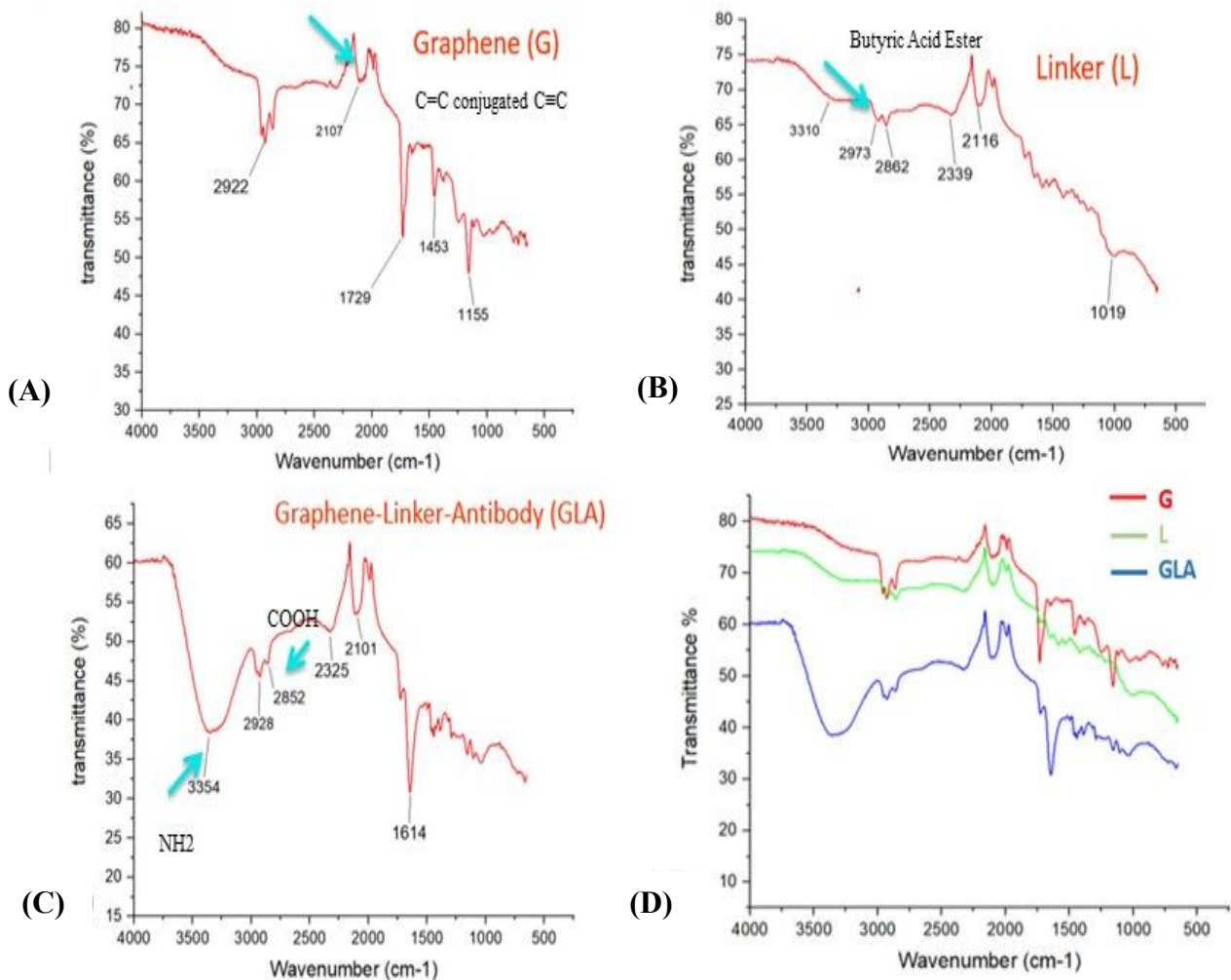
Figure 10:FTIR Analysis (A) Graphene (B) linker (C) GLA (D) Comparison

4.2.4 XRD Analysis

The G sample represented the peaks at 26.7 which indicated the presence of graphene,43.5 showed the presence of silver electrode applied at both ends of the sensor board peaks because of SiO2.In GP one additional peak appeared at 63.8 representing the presence of a linker. There was peak shift appeared in GPA at 38.3 that predicted as presence of antibodies. Shift in peak provided with the confirmation of the presence of antibodies fictionalization on the sensor. The angle of diffraction range was from 0 to 100 while the intensity range was from 0 to1000.
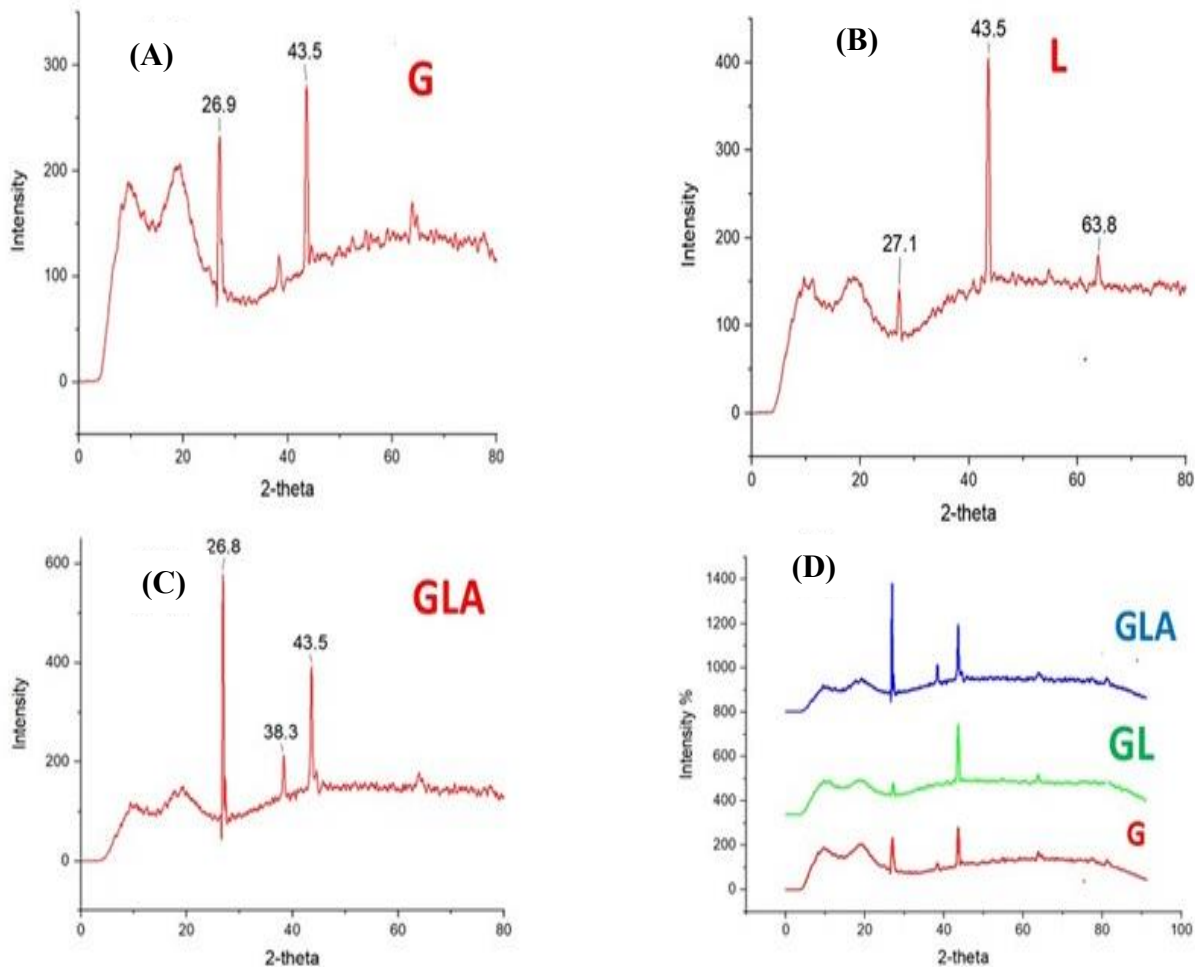
Figure 11:XRD Analysis(A) Graphene (B) linker (C) GLA (D) Comparison

4.2.5. UV Analysis

UV analysis was performed with the help of a microplate reader. Figure no.12 below indicated that graphene sample showed a peak at 269, and PBASE at 344 while there was a peak shift that appeared in the master solution indicating the presence of antibodies. The peak was shifted slightly toward 300. Peaks of graphene appeared as well in the GPA sample.
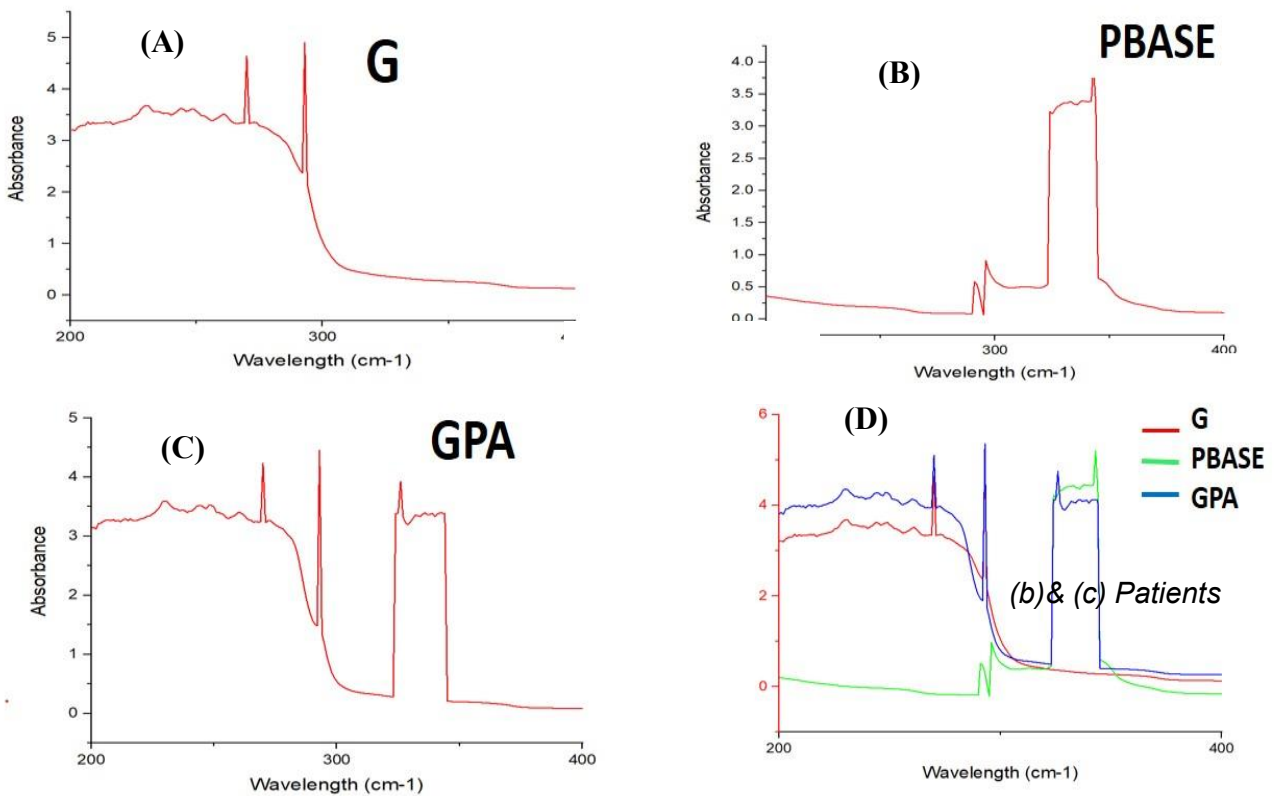
Figure 12: UV- Analysis (A) Graphene (B) linker (C) GLA (D) Comparison

4.2.5 Current-Voltage Measurement

Every material showed a specific current response when a certain range of voltages was applied in linear sweep voltammetry. Non-Conductive substrate showed no response. When the LSV was performed for the control and patient sample, as shown below, some current responses showed up, but the results were unsatisfactory. We will pursue these measurement optimizations in the future.
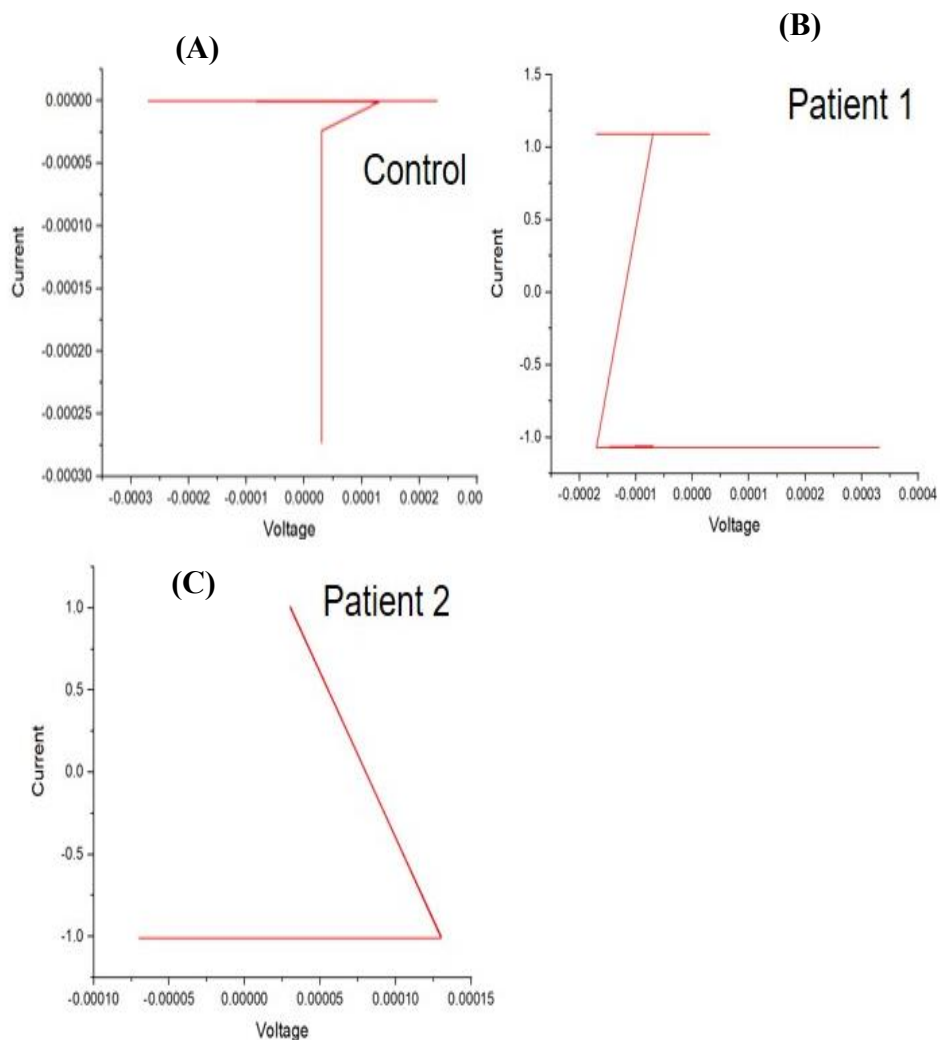
Figure 13: IV Measurements(A) Control (B)& (C) Patients

Chapter 5: Discussion

Cancer costs us millions not in terms of money but also the people we love. Treatment is available for cancer. But the key formula to save people's lives is to diagnose cancer at its earlier stages. The main aim of the study was to develop and characterize the graphene field effect transistor for the diagnosis of cancer. The experimentation and characterization were divided into two parts. Part one was the fabrication of the device while part two comprises the functionalization of the sensor with antibodies. Fabrication mainly consists of coatings and the application of electrodes. The optical profilometry showed an increase in the roughness and height after the coating of SiO2 and graphene coating which confirmed the presence of a coating on our silicon rubber substrate. Roughness, height, and morphological changes were also observed by the 1000X digital microscopy. Those parameters values also represented the coating presence. SiO2 coating was actually used for the purpose of insulator. Because we wanted to obtained voltages value only due changes in graphene layer. For the assurance of SiO2 coating and its insulating properties a dielectric test was performed. Dielectric constant seemed to show inverse relation with presence of binder, as the binder concentration decreased dielectric constant increased. The higher the dielectric constant, the higher the insulating properties of the material. The dielectric constant obtained at 2.5 confirmed the insulating properties of SiO2. Conductance measurement by obtaining the resistance value for both coatings represented the conductive properties of graphene and non-conductive properties of SiO2 by showing some resistance and open loop respectively. Mechanical strength increased after the coating of graphene on SiO2 coating as well as demonstrated the elastic nature of the sensor. Surface analysis of graphene combined with linker and antibodies showed morphological changes showed up under digital microscopy. Similarly, scanning electron microscopy picture demonstrated the immobilization of antibodies on the sensor, as there were white substance linkages showed before the immobilization of antibodies .C=C at2170, ester group at 2973, and NH2 at 3354, and COOH at 2852 in FTIR confirmed the functionalization of the device. XRD analysis gave a peak at 27 for graphene, 43.5 for silver,63.8 for ester, and 38.3 for the antibodies. UV analysis also presented the peaks for graphene at 269 for the linker at 344 while the peak shifted toward 300 in the master solution containing the

antibodies. Linear sweep voltammetry was performed to measure the current response generated by both control and patient over the range of the voltages. But the result wasn't satisfactory, there is still needed to optimize the various parameter regarding the current response measurement to attain the accuracy and efficiency of the device. Graphene-based sensors have drawn a lot of attention because of their outstanding qualities, but they have certain drawbacks as well. Among the main constraints are, environmental sensitivity. Temperature, humidity, and other environmental variables can have an impact on the electrical characteristics of graphene. If not adequately accounted for, this sensitivity may have an impact on the accuracy and reliability of the sensor's measurements. Graphene can be produced using a variety of processes, but it is difficult to get large-area, high-quality graphene. There are still problems that need to be solved regarding the cost-effectiveness and scalability of manufacturing graphene-based sensors for mass applications. Since graphene sensors are typically highly sensitive to a variety of chemicals, they may not have sufficient selectivity for certain analytes. Although graphene by itself is not thought to be harmful, specific functionalization procedures or the presence of impurities may pose toxicity issues, which may restrict its usage in some applications. Due to variations in materials and fabrication techniques, integrating graphene-based sensors into current electrical devices and systems may be difficult. But, despite these limitations of graphene-based sensors, several optimizations are being performed to obtain the required results up to an accuracy.

Chapter 6: Conclusion

Cancer is a leading cause of death worldwide. The incidence and mortality rate of cancer is increasing day by day. Cancer not only increases the economic burden but also leaves us in pain by seeing the sufferings of our beloved. Different treatment strategies are available for cancer. Cancer could be treated if diagnosed at its earlier stages. Currently, available methods for cancer diagnosis are either invasive or late-stage detection methods. One single test for diagnosis of all types of cancer isn't available yet. In our study, we tried to develop and characterize a biosensor for the early diagnosis of all types of cancer.

The main idea was the binding of biomarkers present in serum to the biomarker attached to the sensor. We successfully developed and characterized the sensor. For confirmation of the immobilization of a biomarker on the sensor, FTIR, XRD, SEM, UV, and surface analysis was performed; the results were satisfactory. But the output of current from the input of voltage for cancer patients and the control for proper diagnosis hasn't been optimized yet. The optimization of IV measurements still needed to be done.

6.1 Limitation

The current response to the voltage applied hasn't been measured properly. Optimization is required for this loophole of research. Testing of cancer with many patients is still required for the assurance of the device's proper working. Moreover testing like TEM, AFM, XPM, and XPS are still required to be performed.

6.2 Future Prospects

IV values could be optimized to attain diagnosis optimization. Samples from patients with different types of cancer could be collected and diagnosed with the help of the sensor. Amplifiers could be added for better current measurements. The study could proceed with the different age groups of the people. Sensors could be used for the diagnosis of other diseases as well. Other biomarkers of cancer could also be measured by the device.

References

1. Chaffer, C.L. and R.A. Weinberg, *A perspective on cancer cell metastasis.* science, 2011. **331**(6024): p. 1559-1564.
2. Hakim, D.N., et al., *Benign tumours of the bone: A review.* Journal of bone oncology, 2015. **4**(2): p. 37-41.
3. Wishart, D.S., *Is cancer a genetic disease or a metabolic disease?* EBioMedicine, 2015. **2**(6): p. 478-479.
4. Campisi, J., et al. *Cellular senescence: a link between cancer and age-related degenerative disease?* in *Seminars in cancer biology*. 2011. Elsevier.
5. Williams, C.B., E.S. Yeh, and A.C. Soloff, *Tumor-associated macrophages: unwitting accomplices in breast cancer malignancy.* NPJ breast cancer, 2016. **2**: p. 15025.
6. Barnetson, R.A., et al., *Identification and survival of carriers of mutations in DNA mismatch-repair genes in colon cancer.* New England journal of medicine, 2006. **354**(26): p. 2751-2763.
7. Pfister, S.X. and A. Ashworth, *Marked for death: targeting epigenetic changes in cancer.* Nature reviews Drug discovery, 2017. **16**(4): p. 241-263.
8. Wang, Y.A., et al., *Germline breast cancer susceptibility gene mutations and breast cancer outcomes.* BMC cancer, 2018. **18**: p. 1-13.
9. Martincorena, I. and P.J. Campbell, *Somatic mutation in cancer and normal cells.* Science, 2015. **349**(6255): p. 1483-1489.
10. Almendro, V., A. Marusyk, and K. Polyak, *Cellular heterogeneity and molecular evolution in cancer.* Annual Review of Pathology: Mechanisms of Disease, 2013. **8**: p. 277-302.
11. Temko, D., et al., *The effects of mutational processes and selection on driver mutations across cancer types.* Nature communications, 2018. **9**(1): p. 1857.
12. Roy, D.M., L.A. Walsh, and T.A. Chan, *Driver mutations of cancer epigenomes.* Protein & cell, 2014. **5**(4): p. 265-296.
13. Martínez-Jiménez, F., et al., *A compendium of mutational cancer driver genes.* Nature Reviews Cancer, 2020. **20**(10): p. 555-572.
14. Pon, J.R. and M.A. Marra, *Driver and passenger mutations in cancer.* Annual Review of Pathology: Mechanisms of Disease, 2015. **10**: p. 25-50.
15. McFarland, C.D., et al., *Impact of deleterious passenger mutations on cancer progression.* Proceedings of the National Academy of Sciences, 2013. **110**(8): p. 2910-2915.
16. Siege, L., D. Naishadham, and A. Jemal, *Cancer statistics, 2012.* CA Cancer J Clin, 2012. **62**(1): p. 10-29.
17. Gnad, F., et al., *Assessment of computational methods for predicting the effects of missense mutations in human cancers.* BMC genomics, 2013. **14**(3): p. 1-13.
18. Wood, R.D. and S. Doublié, *DNA polymerase ϑ (POLQ), double-strand break repair, and cancer.* DNA repair, 2016. **44**: p. 22-32.
19. Masetti, R., et al., *Gut microbiome in pediatric acute leukemia: From predisposition to cure.* Blood Advances, 2021. **5**(22): p. 4619-4629.
20. Kim, H., et al., *Melanoma-intrinsic NR2F6 activity regulates antitumor immunity.* Science Advances, 2023. **9**(27): p. eadf6621.
21. Torkamani, A. and N.J. Schork, *Identification of rare cancer driver mutations by network reconstruction.* Genome research, 2009. **19**(9): p. 1570-1578.
22. Kaur, K., et al., *Deficiencies in natural killer cell numbers, expansion, and function at the pre-neoplastic stage of pancreatic cancer by KRAS mutation in the pancreas of obese mice.* Frontiers in immunology, 2018. **9**: p. 1229.

23. Huang, X., G. Zhang, and T. Liang, *Pancreatic tumor initiation: The potential role of IL-33.* Signal Transduction and Targeted Therapy, 2021. **6**(1): p. 204.

24. Park, J.A. and N.-K.V. Cheung, *Limitations and opportunities for immune checkpoint inhibitors in pediatric malignancies.* Cancer treatment reviews, 2017. **58**: p. 22-33.

25. Whatcott, C.J., et al., *Desmoplasia in primary tumors and metastatic lesions of pancreatic cancer.* Clinical Cancer Research, 2015. **21**(15): p. 3561-3568.

26. Riihimäki, M., et al., *Metastatic sites and survival in lung cancer.* Lung cancer, 2014. **86**(1): p. 78-84.

27. Vatandoust, S., T.J. Price, and C.S. Karapetis, *Colorectal cancer: Metastases to a single organ.* World journal of gastroenterology, 2015. **21**(41): p. 11767.

28. Rycaj, K. and D.G. Tang, *Cell-of-origin of cancer versus cancer stem cells: assays and interpretations.* Cancer research, 2015. **75**(19): p. 4003-4011.

29. Pucci, C., C. Martinelli, and G. Ciofani, *Innovative approaches for cancer treatment: Current perspectives and new challenges.* ecancermedicalscience, 2019. **13**.

30. Li, H., X. Wu, and X. Cheng, *Advances in diagnosis and treatment of metastatic cervical cancer.* Journal of gynecologic oncology, 2016. **27**(4).

31. Wender, R., et al., *American Cancer Society lung cancer screening guidelines.* CA: a cancer journal for clinicians, 2013. **63**(2): p. 106-117.

32. Cappello, F., et al., *Exosome levels in human body fluids: A tumor marker by themselves?* European Journal of Pharmaceutical Sciences, 2017. **96**: p. 93-98.

33. Wu, L. and X. Qu, *Cancer biomarker detection: recent achievements and challenges.* Chemical Society Reviews, 2015. **44**(10): p. 2963-2997.

34. Proust-Lima, C., et al., *Confirmation of a low α/β ratio for prostate cancer treated by external beam radiation therapy alone using a post-treatment repeated-measures model for PSA dynamics.* International Journal of Radiation Oncology* Biology* Physics, 2011. **79**(1): p. 195-201.

35. Gudmundsson, J., et al., *Genome-wide associations for benign prostatic hyperplasia reveal a genetic correlation with serum levels of PSA.* Nature communications, 2018. **9**(1): p. 4568.

36. Ito, K., et al., *Diagnostic significance of [− 2] pro-PSA and prostate dimension-adjusted PSA-related indices in men with total PSA in the 2.0–10.0 ng/mL range.* World journal of urology, 2013. **31**: p. 305-311.

37. Ost, P., et al., *Prognostic factors influencing prostate cancer-specific survival in non-castrate patients with metastatic prostate cancer.* The Prostate, 2014. **74**(3): p. 297-305.

38. Hoffman, R.M., *Screening for prostate cancer.* New England Journal of Medicine, 2011. **365**(21): p. 2013-2019.

39. Karam, A.K. and B.Y. Karlan, *Ovarian cancer: the duplicity of CA125 measurement.* Nature reviews Clinical oncology, 2010. **7**(6): p. 335.

40. Zhang, M., et al., *Roles of CA125 in diagnosis, prediction, and oncogenesis of ovarian cancer.* Biochimica et Biophysica Acta (BBA)-Reviews on Cancer, 2021. **1875**(2): p. 188503.

41. Hu, C.-M.J., et al., *Half-antibody functionalized lipid– polymer hybrid nanoparticles for targeted drug delivery to carcinoembryonic antigen presenting pancreatic cancer cells.* Molecular pharmaceutics, 2010. **7**(3): p. 914-920.

42. Pavlopoulou, A. and A. Scorilas, *A comprehensive phylogenetic and structural analysis of the carcinoembryonic antigen (CEA) gene family.* Genome biology and evolution, 2014. **6**(6): p. 1314-1326.

43. Zheng, L., et al., *Effects of AFP-activated PI3K/Akt signaling pathway on cell proliferation of liver cancer.* Tumor Biology, 2014. **35**: p. 4095-4099.

44.   He, Y., H. Lu, and L. Zhang, *Serum AFP levels in patients suffering from 47 different types of cancers and noncancer diseases.* Progress in molecular biology and translational science, 2019. **162**: p. 199-212.

45.   Nasioudis, D., et al., *Management and prognosis of ovarian yolk sac tumors; an analysis of the National Cancer Data Base.* Gynecologic Oncology, 2017. **147**(2): p. 296-301.

46.   Smith, Z.L., R.P. Werntz, and S.E. Eggener, *Testicular cancer: epidemiology, diagnosis, and management.* Medical Clinics, 2018. **102**(2): p. 251-264.

47.   Favilla, V., et al., *New advances in clinical biomarkers in testis cancer.* Frontiers in Bioscience-Elite, 2010. **2**(2): p. 456-477.

48.   Fabian, A. and R. Ross, *X-ray Reflection.* Space science reviews, 2010. **157**: p. 167-176.

49.   Yu, C., et al., *The potential of terahertz imaging for cancer diagnosis: A review of investigations to date.* Quantitative imaging in medicine and surgery, 2012. **2**(1): p. 33.

50.   Biswas, S., et al., *Anti-transforming growth factor ss antibody treatment rescues bone loss and prevents breast cancer metastasis to bone.* PloS one, 2011. **6**(11): p. e27090.

51.   Allen, V.B., et al., *Diagnostic accuracy of laparoscopy following computed tomography (CT) scanning for assessing the resectability with curative intent in pancreatic and periampullary cancer.* Cochrane Database of Systematic Reviews, 2016(7).

52.   McCollough, C.H., et al., *Dual-and multi-energy CT: principles, technical approaches, and clinical applications.* Radiology, 2015. **276**(3): p. 637-653.

53.   Firmino, M., et al., *Computer-aided detection system for lung cancer in computed tomography scans: review and future prospects.* Biomedical engineering online, 2014. **13**(1): p. 1-16.

54.   Almuhaideb, A., N. Papathanasiou, and J. Bomanji, *18F-FDG PET/CT imaging in oncology.* Annals of Saudi medicine, 2011. **31**(1): p. 3-13.

55.   Brown, M.A. and R.C. Semelka, *MRI: basic principles and applications*. 2011: John Wiley & Sons.

56.   Grover, V.P., et al., *Magnetic resonance imaging: principles and techniques: lessons for clinicians.* Journal of clinical and experimental hepatology, 2015. **5**(3): p. 246-255.

57.   Westbrook, C. and J. Talbot, *MRI in Practice*. 2018: John Wiley & Sons.

58.   Disselhorst, J.A., et al., *Principles of PET/MR imaging.* Journal of Nuclear Medicine, 2014. **55**(Supplement 2): p. 2S-10S.

59.   Saha, G.B., *Basics of PET imaging: physics, chemistry, and regulations*. 2015: Springer.

60.   Zanzonico, P., *Principles of nuclear medicine imaging: planar, SPECT, PET, multi-modality, and autoradiography systems.* Radiation research, 2012. **177**(4): p. 349-364.

61.   Gennisson, J.-L., et al., *Ultrasound elastography: principles and techniques.* Diagnostic and interventional imaging, 2013. **94**(5): p. 487-495.

62.   Jalalian, A., et al., *Computer-aided detection/diagnosis of breast cancer in mammography and ultrasound: a review.* Clinical imaging, 2013. **37**(3): p. 420-426.

63.   Lee, H., J. Park, and J.Y. Hwang, *Channel attention module with multiscale grid average pooling for breast cancer segmentation in an ultrasound image.* IEEE transactions on ultrasonics, ferroelectrics, and frequency control, 2020. **67**(7): p. 1344-1353.

64.   Larkin, J., et al., *Combined electric field and ultrasound therapy as a novel anti-tumour treatment.* European Journal of Cancer, 2005. **41**(9): p. 1339-1348.

65.   Khuri-Yakub, B.T., O. Oralkan, and M. Kupnik, *Next-gen ultrasound.* iEEE SpEctrum, 2009. **46**(5): p. 44-54.

66.   Enneking, W.F., *The issue of the biopsy.* JBJS, 1982. **64**(8): p. 1119-1120.

67.   Palmirotta, R., et al., *Liquid biopsy of cancer: a multimodal diagnostic tool in clinical oncology.* Therapeutic advances in medical oncology, 2018. **10**: p. 1758835918794630.

68.   Pandharipande, P.V., et al., *Renal mass biopsy to guide treatment decisions for small incidental renal tumors: a cost-effectiveness analysis.* Radiology, 2010. **256**(3): p. 836-846.

69. Rubio, I.T., et al., *Sentinel lymph node biopsy for staging breast cancer.* The American journal of surgery, 1998. **176**(6): p. 532-537.

70. Parker, S.H., A.T. Stavros, and M.A. Dennis, *Needle biopsy techniques.* Radiologic Clinics of North America, 1995. **33**(6): p. 1171-1186.

71. Levy, I. and I.M. Gralnek, *Complications of diagnostic colonoscopy, upper endoscopy, and enteroscopy.* Best practice & research Clinical gastroenterology, 2016. **30**(5): p. 705-718.

72. Buselli, E., et al., *Evaluation of friction enhancement through soft polymer micro-patterns in active capsule endoscopy.* Measurement Science and Technology, 2010. **21**(10): p. 105802.

73. Watmough, S. and M. Flynn, *A review of pain management interventions in bone marrow biopsy.* Journal of clinical nursing, 2011. **20**(5-6): p. 615-623.

74. El-Galaly, T.C., et al., *Routine bone marrow biopsy has little or no therapeutic consequence for positron emission tomography/computed tomography–staged treatment-naive patients with Hodgkin lymphoma.* Journal of clinical oncology, 2012. **30**(36): p. 4508-4514.

75. Bruening, W., et al., *Systematic review: comparative effectiveness of core-needle and open surgical biopsy to diagnose breast lesions.* Annals of internal medicine, 2010. **152**(4): p. 238-246.

76. Kasraeian, S., et al., *A comparison of fine-needle aspiration, core biopsy, and surgical biopsy in the diagnosis of extremity soft tissue masses.* Clinical Orthopaedics and Related Research®, 2010. **468**: p. 2992-3002.

77. Ali, J., et al., *Biosensors: their fundamentals, designs, types and most recent impactful applications: a review.* J. Biosens. Bioelectron, 2017. **8**(1): p. 1-9.

78. Peña-Bahamonde, J., et al., *Recent advances in graphene-based biosensor technology with applications in life sciences.* Journal of nanobiotechnology, 2018. **16**: p. 1-17.

79. Abergel, D., et al., *Properties of graphene: a theoretical perspective.* Advances in Physics, 2010. **59**(4): p. 261-482.

80. Fu, W., et al., *Sensing at the surface of graphene field-effect transistors.* Advanced Materials, 2017. **29**(6): p. 1603610.

81. Haslam, C., et al., *Label-free sensors based on graphene field-effect transistors for the detection of human chorionic gonadotropin cancer risk biomarker.* Diagnostics, 2018. **8**(1): p. 5.

82. Fenoy, G.E., et al., *Acetylcholine biosensor based on the electrochemical functionalization of graphene field-effect transistors.* Biosensors and Bioelectronics, 2020. **148**: p. 111796.

83. Ferlay, J., et al., *Cancer statistics for the year 2020: An overview.* International journal of cancer, 2021. **149**(4): p. 778-789.

84. Jang, S.J., J.M. Gardner, and J.Y. Ro, *Diagnostic approach and prognostic factors of cancers.* Advances in anatomic pathology, 2011. **18**(2): p. 165-172.

85. Gholve, C., et al., *Comparison of serum thyroglobulin levels in differentiated thyroid cancer patients using In-house developed radioimmunoassay and immunoradiometric procedures.* Indian Journal of Clinical Biochemistry, 2019. **34**: p. 465-471.

86. Ravaioli, S., et al., *Easily detectable cytomorphological features to evaluate during ROSE for rapid lung cancer diagnosis: from cytology to histology.* Oncotarget, 2017. **8**(7): p. 11199.

87. Hassan, S., et al., *Diagnostic and Therapeutic Potential of Circulating-Free DNA and Cell-Free RNA in Cancer Management. Biomedicines 2022, 10, 2047.* 2022, s Note: MDPI stays neutral with regard to jurisdictional claims in published ….

88. Zhang, Q., et al. *Detection of exosomes using liquid-gated graphene field effect transistor biosensors*. in *2021 15th International Conference on Advanced Technologies, Systems and Services in Telecommunications (TELSIKS)*. 2021. IEEE.

89. Zhang, X., et al., *Electrical probing of COVID-19 spike protein receptor binding domain via a graphene field-effect transistor.* arXiv preprint arXiv:2003.12529, 2020.

90. Selvarajan, R.S., et al., *Ultrasensitive and highly selective graphene-based field-effect transistor biosensor for anti-diuretic hormone detection.* Sensors, 2020. **20**(9): p. 2642.

Areej

13%	10%	6%	5%
SIMILARITY INDEX	INTERNET SOURCES	PUBLICATIONS	STUDENT PAPERS

PRIMARY SOURCES

1. www.ncbi.nlm.nih.gov
Internet Source — 1%

2. Michael R. Stratton. "Exploring the Genomes of Cancer Cells: Progress and Promise", Science, 2011
Publication — 1%

3. science.sciencemag.org
Internet Source — 1%

4. sist.sathyabama.ac.in
Internet Source — 1%

5. www.science.gov
Internet Source — 1%

6. Submitted to Abu Dhabi University
Student Paper — 1%

7. www.santi-shop.eu
Internet Source — <1%

8. training.seer.cancer.gov
Internet Source — <1%

9   Changhao Dai, Yunqi Liu, Dacheng Wei. "Two-Dimensional Field-Effect Transistor Sensors: The Road toward Commercialization", Chemical Reviews, 2022
Publication
<1%

10 pubmed.ncbi.nlm.nih.gov
Internet Source
<1%

11 www.drugs.com
Internet Source
<1%

12 dc.uwm.edu
Internet Source
<1%

13 pesquisa.bvsalud.org
Internet Source
<1%

14 Submitted to University of Wisconsin, La Crosse
Student Paper
<1%

15 Submitted to Weber State University
Student Paper
<1%

16 ncbi.nlm.nih.gov
Internet Source
<1%

17 www.mdpi.com
Internet Source
<1%

18 Submitted to The Jannali High School
Student Paper
<1%

trepo.tuni.fi

19	Internet Source	<1%
20	Submitted to Solihull College, West Midlands Student Paper	<1%
21	rcastoragev2.blob.core.windows.net Internet Source	<1%
22	Submitted to College of Haringey, Enfield and North East London Student Paper	<1%
23	Submitted to International Islamic University Malaysia Student Paper	<1%
24	Submitted to Chippewa Valley Schools Student Paper	<1%
25	Submitted to University of Exeter Student Paper	<1%
26	patents.google.com Internet Source	<1%
27	www.researchgate.net Internet Source	<1%
28	www2.mdpi.com Internet Source	<1%
29	Submitted to Pembroke School Student Paper	<1%

30	sunridgemedical.com Internet Source	<1%
31	Submitted to York Technical College Student Paper	<1%
32	B. Vogelstein, N. Papadopoulos, V. E. Velculescu, S. Zhou, L. A. Diaz, K. W. Kinzler. "Cancer Genome Landscapes", Science, 2013 Publication	<1%
33	www.coursehero.com Internet Source	<1%
34	Submitted to Jyväskyla University Student Paper	<1%
35	Submitted to Sir George Monoux College Student Paper	<1%
36	Submitted to Laureate Higher Education Group Student Paper	<1%
37	Sadia Hassan, Aroosa Younis Nadeem, Muhammad Ali, Murtaza Najabat Ali, Muhammad Bilal Khan Niazi, Azhar Mahmood. "Graphite coatings for biomedical implants: A focus on anti-thrombosis and corrosion resistance properties", Materials Chemistry and Physics, 2022 Publication	<1%

Submitted to United Colleges Group - UCG

30	sunridgemedical.com Internet Source	<1%
31	Submitted to York Technical College Student Paper	<1%
32	B. Vogelstein, N. Papadopoulos, V. E. Velculescu, S. Zhou, L. A. Diaz, K. W. Kinzler. "Cancer Genome Landscapes", Science, 2013 Publication	<1%
33	www.coursehero.com Internet Source	<1%
34	Submitted to Jyväskyla University Student Paper	<1%
35	Submitted to Sir George Monoux College Student Paper	<1%
36	Submitted to Laureate Higher Education Group Student Paper	<1%
37	Sadia Hassan, Aroosa Younis Nadeem, Muhammad Ali, Murtaza Najabat Ali, Muhammad Bilal Khan Niazi, Azhar Mahmood. "Graphite coatings for biomedical implants: A focus on anti-thrombosis and corrosion resistance properties", Materials Chemistry and Physics, 2022 Publication	<1%

Submitted to United Colleges Group - UCG

44 Submitted to Ain Shams University
Student Paper
<1%

45 Lingzhi Zhao. "CD33 in Alzheimer's Disease –
Biology, Pathogenesis, and Therapeutics: A
Mini-Review", Gerontology, 2019
Publication
<1%

46 Submitted to Ramapo College
Student Paper
<1%

47 Scott W. Piraino, Valentina Thomas, Peter
O'Donovan, Simon J. Furney. "Driver Versus
Passenger Mutations in Tumors", Elsevier BV,
2018
Publication
<1%

48 epdf.pub
Internet Source
<1%

49 hellodoctor.com.ph
Internet Source
<1%

50 theswissbay.ch
Internet Source
<1%

51 Ahmad Taher Azar, Shereen M. El-Metwally.
"Decision tree classifiers for automated
medical diagnosis", Neural Computing and
Applications, 2012
Publication
<1%

52 doaj.org
Internet Source
<1%

Reena Sri Selvarajan, Ruslinda A. Rahim, Burhanuddin Yeop Majlis, Subash C. B. Gopinath, Azrul Azlan Hamzah. "Ultrasensitive and Highly Selective Graphene-Based Field-Effect Transistor Biosensor for Anti-Diuretic Hormone Detection", Sensors, 2020
Publication

<1 %

Exclude quotes   Off

Exclude matches   Off